Revision of basal macropodids from the Riversleigh World Heritage Area with descriptions of new material of *Ganguroo bilamina* Cooke, 1997 and a new species

K.J. Travouillon, B.N. Cooke, M. Archer, and S.J. Hand

ABSTRACT

The relationship of basal macropodids (Marsupialia: Macropodoidea) from the Oligo-Miocene of Australia have been unclear. Here, we describe a new species from the Bitesantennary Site within the Riversleigh's World Heritage Area (WHA), *Ganguroo bites* n. sp., new cranial and dental material of *G. bilamina,* and reassess material previously described as *Bulungamaya delicata* and '*Nowidgee matrix'.* We performed a metric analysis of dental measurements on species of *Thylogale* which we then used, in combination with morphological features, to determine species boundaries in the fossils. We also performed a phylogenetic analysis to clarify the relationships of basal macropodid species within Macropodoidea. Our results support the distinction of *G. bilamina, G. bites* and *B. delicata,* but '*Nowidgee matrix'* appears to be a synonym of *B. delicata.* The results of our phylogenetic analysis are inconclusive, but dental and cranial features suggest a close affinity between *G. bilamina* and macropodids. Finally, we revise the current understanding of basal macropodid diversity in Oligocene and Miocene sites at Riversleigh WHA.

K.J. Travouillon. School of Earth Sciences, University of Queensland, St Lucia, Queensland 4072, Australia and School of Biological, Earth and Environmental Sciences, University of New South Wales, New South Wales 2052, Australia. k.travouillon@uq.edu.au
B.N. Cooke. Queensland Museum, PO Box 3300, South Brisbane, Queensland 4101, Australia. bncooke@bigpond.net.au
M. Archer. School of Biological, Earth and Environmental Sciences, University of New South Wales, New South Wales 2052, Australia. m.archer@unsw.edu.au
S.J. Hand. School of Biological, Earth and Environmental Sciences, University of New South Wales, New South Wales 2052, Australia. s.hand@unsw.edu.au

INTRODUCTION

Archer (1979) described the first macropodoid from the Riversleigh World Heritage Area (WHA), *Wabularoo naughtoni*, on the basis of a single dentary found at D Site. It differed from potoroines in having bilophodont molars, and from macropodids in having an enlarged masseteric canal, but shares with both a tall and wide plagiaulacoid p3. Flannery et al. (1983) identified an additional left p3 of *W. naughtoni* from the Riversleigh's G Site and erected a new potoroid (their potoroines) subfamily, 'Bulungamayinae', to accomodate *W. naughtoni* and a new species, *Bulungamaya delicata.* The latter was described from damaged, heavily worn dentaries found at D Site and G Site. It is smaller than *W. naughtoni*, has less well-developed lophids (although heavily obscured by wear) and a posthypocristid at least on m3 (their m4; other molars were too worn to tell). Case (1984) and Woodburne (1984) suggested *B. delicata* and *W. naughtoni* represent macropodids (their macropodines) rather than potoroids, but Flannery et al. (1984) provided further evidence for their original assignation based on an additional dentary of *W. naughtoni* from D Site.

Cooke (1997a) described two new macropodoid species from Riversleigh WHA, *'Nowidgee matrix'* and *Ganguroo bilamina. 'Nowidgee matrix'* is clearly bunolophodont (sensu Flannery et al., 1984), with the buccally-directed cristid from the entoconid forming the hypolophid. The cristid obliqua is also well-developed in this species and ascends to the apex of the protoconid. In contrast, *G. bilamina* is completely bilophodont, the hypolophid crest being formed entirely by the much elevated posthypocristid, the posterior cingulid being lost and no trace remains of a buccal cristid associated with the entoconid apex. Cooke (1997a) also discussed differences between *Bulungamaya delicata, 'N. matrix'* and *G. bilamina.* Additional material referable to *B. delicata* was reported from a number of Riversleigh local faunas (LFs) in Faunal Zones B and C (Cooke, 1997b; Archer et al., 2006). Some of these specimens have been used in phylogenetic analyses (Kear and Cooke, 2001; Kear et al., 2001a; Kear et al., 2007; Kear and Pledge, 2008). However, none of these specimens have been described. We also question their assignment to *B. delicata.* Upper molars with a clearly bunolophodont morphology have been confidently assigned to *N. matrix* (Cooke, 1997a) but upper molars of *B. delicata* and *G. bilamina* have yet to be recognised. Considerable numbers of maxillae and even partial skulls of small macropo-

dids of a size range appropriate for either *B. delicata* or *G. bilamina* have now been recovered from Riversleigh. Unfortunately none of these involves unambiguously associated upper and lower dentitions. Similarities in morphology of associated specimens (skulls and dentaries) from a small macropodid species from Faunal Zone C, *Ganguroo* sp. 2 (Cooke, 1997b; Archer et al., 2006), suggest that all maxillae and partial skulls recovered to date from Faunal Zone B are likely to belong to *G. bilamina.* These specimens are described in the current paper. Previous phylogenetic analyses have also used postcranial characters for *G. bilamina* based on specimens from the middle Miocene AL90 Site (Kear et al., 2001a). However, these postcranials were found in association with unnamed species *Ganguroo* sp. 2, not *G. bilamina.* In view of previous confusion and the description here of additional materials that increase understanding about basal macropodid taxa, we have conducted a new phylogenetic analysis for *B. delicata, N. matrix*, *G. bilamina* and *G. bites* n. sp. from Bitesantennary LF. Finally, we reassess the diversity of taxa currently known from the Riversleigh WHA.

MATERIALS AND METHODS

Materials and Dental Measurements

Specimens of *Bulungamaya delicata, 'Nowidgee matrix', Ganguroo bilamina* and *G. bites* n. sp. used in this study were collected from fossil sites in the Riversleigh World Heritage Area, northwestern Queensland (18°59'-19°08'S, 138°34'-138°43'E). Specimens with the prefix QM F are from the Queensland Museum fossil collection, Brisbane, Australia. One specimen of *G. bilamina* in the fossil collections of the University of California at Berkeley (UCMP) was recovered from the Wipajiri Formation at the Leaf Locality, Lake Ngapakaldi, South Australia. Other specimens from the Etadunna Formation of South Australia in the collections of the South Australian Museum (SAM P) used in metric analyses represent *Ngamaroo archeri* (Kear and Pledge, 2008) and *Purtia mosaicus* (Case, 1984). Specimens of the modern Red-legged Pademelon (*Thylogale stigmatica*) and Red-necked Pademelon (*Thylogale thetis*) were examined from the Queensland Museum mammal collection (QM J or JM).

All specimens were measured using digital vernier callipers. Maximum anteroposterior length and buccolingual width measurements of deciduous and adult premolars were made at the base of

the crown. Width measurements for molars were measured across the anterior and posterior lophs/lophids. All specimens examined and their measurements are provided in Appendices 1, 2, 3, 4, 5, 6 and 7.

Metric Analysis

All metric analyses were performed using the computer software PAST Version 1.51 (Hammer et al., 2001). To assess the amount of variation in upper and lower premolars and molars in modern macropodoids, basic univariate statistics were calculated for *Thylogale stigmatica* and *Thylogale thetis*. These two taxa were chosen because they are congeneric, have very similar dental morphology and are sympatric. Intraspecific dental variation in these species may help to illuminate species boundaries within the fossil samples. In order to assess the potential for failure to recognise distinct species in the fossil samples, basic univariate statics were calculated for combined measurements of *Thylogale stigmatica* + *Thylogale thetis.* Bivariate plots of tooth measurements (length versus anterior or posterior width), for males and females in each taxon were also generated. Principle Component Analyses (PCAs) were performed using the same measurements, log transformed, to assess which dental measurements appeared to distinguish these two taxa. A Multivariate Analysis of Variance (MANOVA) was performed to test whether the means of the log transformed dental measurements were statistically different between sexes of each species and between species. A Canonical Variates Analysis (CVA) was also used to produce a scatter plot of specimens along the two canonical axes, producing maximal and second to maximal separation between all groups (multigroup discriminant analysis), which is then able to reclassify specimens. This method is used here as a way to test whether fossil specimens would be able to correctly reclassify with the correct taxon using log transformed dental measurements.

Basic univariate statistics were also calculated for *G. bilamina* (*G. bites* sample size too small to include*)* and *B. delicata* + *N. matrix*. Bivariate plots, PCAs, MANOVAs, and CVAs were repeated for all fossil taxa listed above.

Terminology

Cheek-tooth homology follows Flower (1869) and Luckett (1993). Dental terminology follows Archer (1984), Tedford and Woodburne (1987), Szalay (1969) and Cooke (1997a, 1997b). Systematic nomenclature follows Aplin and Archer (1987) and Kear and Cooke (2001) for higher-level marsupial relationships. Cranial terminology follows Wible (2003) and Murray (1989).

Biostratigraphic nomenclature follows Archer et al. (1989, 1997), Creaser (1997), Arena (2004) and Travouillon et al. (2006, 2011).

Phylogenetic Analyses

We assessed the phylogenetic relationships of basal macropodid species to other macropodoids using the matrix of Kear and Pledge (2008). While the matrix of Prideaux and Warburton (2010) is more recent, they acknowledged that their principle purpose was to investigate the relationship of bilophodont macropodids, and therefore not suitable to analyse more basal forms. They mentioned that their matrix would require an extensive increase in characters and additional outgroups before it could be used for that purpose. Hence why we used the matrix of Kear and Pledge (2008), because it was explicitly generated for assessing the relationship of basal macropodiforms. Their matrix contained 108 qualitative morphological characters including cranial, dental and postcranial features. We removed skull and upper dentition scores for *Wabularoo naughtoni* because material scored previously was unpublished and may represent a different species. Only the holotype of that species, QM F9177 (Archer, 1979) which is a dentary containing p3 m1-3, was used to score characters. We scored the new specimens of *Ganguroo bilamina*, which included cranial and upper dentition characters, and removed postcranial scores for *G. bilamina* because the postcranials described by Kear et al. (2001a) belong to a different species of *Ganguroo* found in Riversleigh's Faunal Zone C (see *Ganguroo* sp. 2 in Archer et al., 2006). Several skulls and dentaries from the AL90 Site that were associated with postcranials will be described shortly (Cooke et al., in review). The new *Ganguroo* species from the Bitesantennary Site described in this paper was also scored and added to the matrix. Finally, we deleted '*Nowidgee matrix*' from the matrix (see discussion) and rescored *Bulungamaya delicata* based only on the material assigned to this species in the current paper.

A parsimony analysis was performed following Worthy et al. (2006) and Beck et al. (2008) with PAUP* 4.0b10 (Swofford, 2002) using a two-stage search strategy. An initial search comprising 1,000 heuristic replicates, saving 10 trees per replicate, was followed by a second heuristic search within the saved trees. This method allows optimising the

heuristic search and minimising the number of most parsimonious trees. All most parsimonious tress produced were summarised as a strict consensus tree. Bootstrap values for each node were calculated using 1000 bootstrap replicates of 10 random addition sequence replicates and decay indices were also calculated using TreeRot.v3 (Sorenson and Franzosa, 2007).

SYSTEMATIC PALAEONTOLOGY

Family MACROPODIDAE Gray, 1821
Genus *GANGUROO* Cooke, 1997a

Type Species.- *Ganguroo bilamina* Cooke, 1997a
Additional Species.- *G. bites* n. sp.
Revised Generic Diagnosis. Species of *Ganguroo* differ from all hypsiprimnodontids and potoroines by having bilophodont molars and m4 is not greatly reduced in size relative to other molars. They differ from all macropodines and sthenurines by having a combination of: a buccally expanded masseteric canal; a sharp ventrally convex dentary margin below m1-2; i1 with enamel confined to the buccal surface and extensive on that surface; ventral and dorsal flanges present on i1; p3 and P3 elongate with fine transcristids and a bulbous base; a small precingulid present anterobuccal to the paracristid; lower molars and dp3 bilophodont. It differs from balbarids in lacking a posterior cingulid on any lower molars and m1 lacks a protostylid (Kear and Cooke, 2001).
Remarks. A third species of *Ganguroo*, referred to in Cooke, 1997b (and consequently in Archer et al., 2006; Travouillon et al., 2006, 2009, 2011) as *Ganguroo* sp. 2, has yet to be described. This species seems to be common but restricted to Faunal Zones C and D Sites at Riversleigh.

Ganguroo bilamina, Cooke, 1997a
Figures 1, 2, 3, 4

Revised Species Diagnosis. *Ganguroo bilamina* is characterised by the following features: flat frontal region; broad parietal-alisphenoid contact; alisphenoid contribution to ventral floor of secondary foramen ovale; carotid foramen anterior to posterior margin of basisphenoid; upper canines present; P3 elongate with a bulbous base and 7 cusps and associated transcristae (in more worn specimens, the 7th and sometimes even the 6th cusps/transcristae are worn off); upper molars and dP3 bilophodont; stylar cusp C present on all upper molars but decreases in size posteriorly; protoloph in upper molars formed mainly by the preprotocrista and always joins to preparacrista, but also forms a small forelink anteriorly; neometaconule

and associated crest (postlink) present on dP3 and all upper molars, decreasing in size posteriorly (presence may be affected by wear); and small alveolus for i2 present directly posterior to i1.

Ganguroo bilamina differs from *G. bites* in: having 7 cuspids and associated transcristids (contra Cooke, 1997a) on p3 (instead of 8 in *G. bites*); a shorter and wider p3; smaller and narrower lower molars that are rectangular in occlusal outline; paraconid absent; and a buccal crest from the entoconid in some juveniles (contra Cooke, 1997a).
Holotype. QM F19915, left dentary with i1, p3, m1-4.
Referred Material. From Riversleigh WHA, Cadbury's Kingdom Site: QM F56318, left P3; Camel Sputum Site: QM F19870, left dentary with m1-4, QM F19868, left dentary with i1, p3, m2-3, QM F19966, left dentary with p3, m1-4, QM F30400, left dentary with m2-4, QM F56996, left dentary with dp3, p3, m1-3, m4 in crypt, QM F19607, left dentary with p3, m1-3, QM F20248, right dentary with dp2-3, m1, QM F20254, right dentary with m4, QM F23486, right dentary with worn m2-4, QM F20246, right dentary with p3, QM F20019, left dentary with dp2, m1, QM F56994, left dentary with p3, QM F19903, left dentary with i1, dp2-3, p3, m1-3, QM F56254, right dentary with i1, dp2-3, p3, m1-3, QM F56259, right dentary with p3, m1-4, QM F24744, right dentary with dp2-3, m1-3, QM F56995, right maxilla with dP3, P3, M1, QM F19696, skull with right and left P3, M1-3, QM F19958, left maxilla with M1-3, QM F20705, left maxilla with P3, M1-2, broken M3, QM F19900, left maxilla with M1-4, QM F19695, left maxilla with P3, M1-2, QM F20253, right maxilla with P3, M1, broken M2, QM F19861, left maxilla with dP2-3, M1-3, QM F19976, left maxilla with dP2-3, M1, QM F19957, left maxilla with broken M1, M2-4, QM F19857, right maxilla with dP2-3, M1-3, QM F19975, left maxilla with M1-3, QM F19959, left maxilla with M2-3, QM F20017, right maxilla with P3, M1-4, QM F56990, left maxilla with broken M2-3, M4, QM F30436, left maxilla with M1-3, QM F30343, left maxilla with dP2-3, M1-2, QM F36230, right maxilla with M1-3; Inabeyance Site: QM F20006, left dentary with dp2, p3, m1-3; Judith's Horizontalis Site: QM F36351, right dentary with i1, p3, m1-4; Mike's Menagerie Site: QM F19988, right dentary with m3-4, QM F19844, left dentary with m1-2, QM F19668, right maxilla with M1-2, QM F19692, right maxilla with M1-4; Mike's Potato Patch Site: QM F234604, left maxilla with dP2, M1; Neville's Garden Site: QM F24190, right dentary
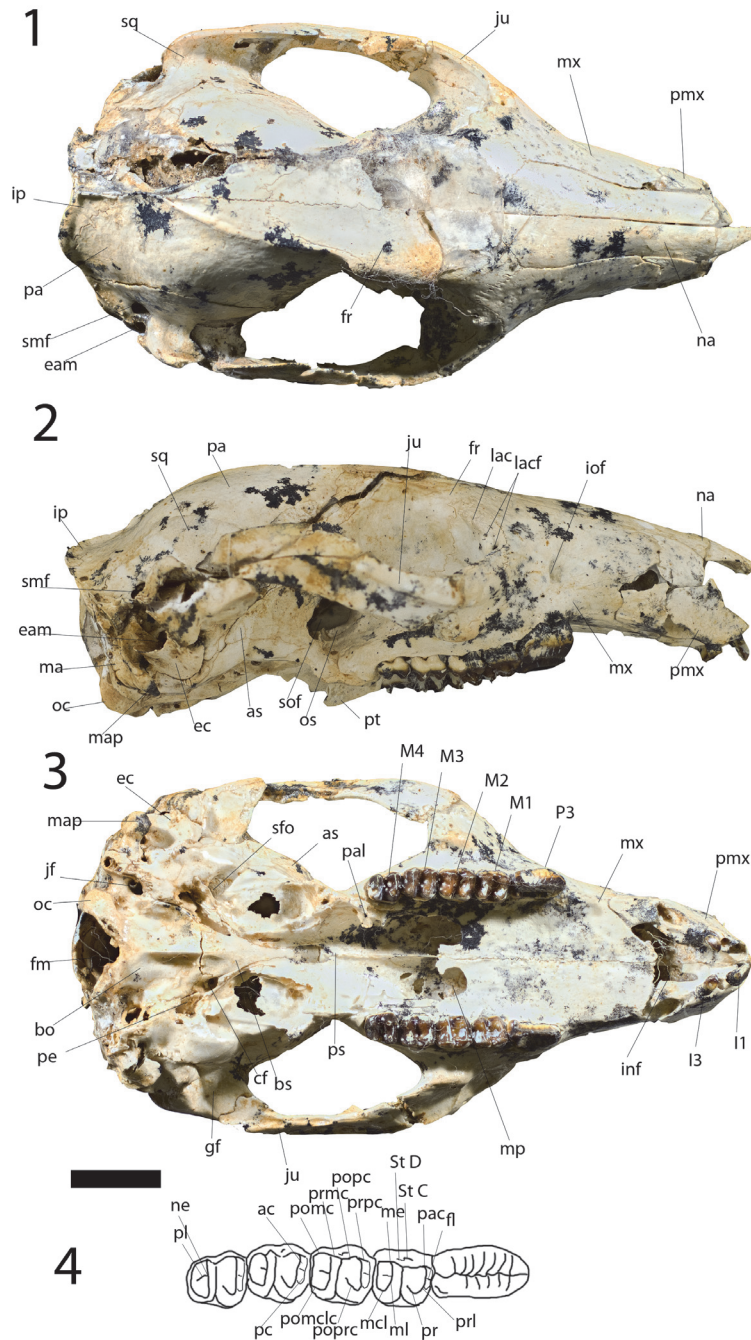
FIGURE 1. *Ganguroo bilamina* skull (QM F56265) from Wayne's Wok Site, in dorsal (**1**), right lateral (**2**) and ventral (**3**) views. (**4**) Line drawing of the upper right cheek teeth of QM F56265. **Abbreviations**: **ac**, anterior cingulum; **as**, alisphenoid; **bo**, basioccipital; **bs**, basisphenoid; **cf**, carotid foramen; **eam**, external auditory meatus; **ec**, ectotympanic; **fl**, forelink; **fm**, foramen magnum; **fr**, frontal; **gf**, glenoid fossa; **iof**, infraorbital foramen; **I1, I3**, upper incisor one and three; **inf**, incisive fenestra; **ip**, interparietal; **jf**, jugular foramen; **ju**, jugal; **lac**, lacrimal; **lacf**, lacrimal foramen; **M1-M4**, upper molar one to molar four; **ma**, mastoid; **map**, mastoid process; **mcl**, metaconule; **me**, metacone; **ml**, metaloph; **mp**, maxillopalatine fenestra; **mx**, maxilla; **na**, nasal; **ne**, neometaconule; **oc**, occipital condyle; **os,** orbitosphenoid; **P3,** upper third premolar; **pa**, parietal; **pac**, paracone; **pal**, palatine; **pc**, precingulum; **pe**, petrosal; **pl**, postlink; **pmx**, premaxilla; **pomc**, postmetacrista; **pomclc**, postmetaconulecrista; **popc**, postparacrista; **poprc**, postprotocrista; **pr**, protocone; **prl**, protoloph; **prmc**, premetacrista; **prpc**, preparacrista; **ps**, presphenoid; **pt**, pterygoid; **sfo**, secondary foramen ovale; **smf**, suprameatal foramen; **sof,** sphenorbital fissure; **sq**, squamosal; **St C-D**, stylar cusp C and D. Scale bar equals 10 mm.
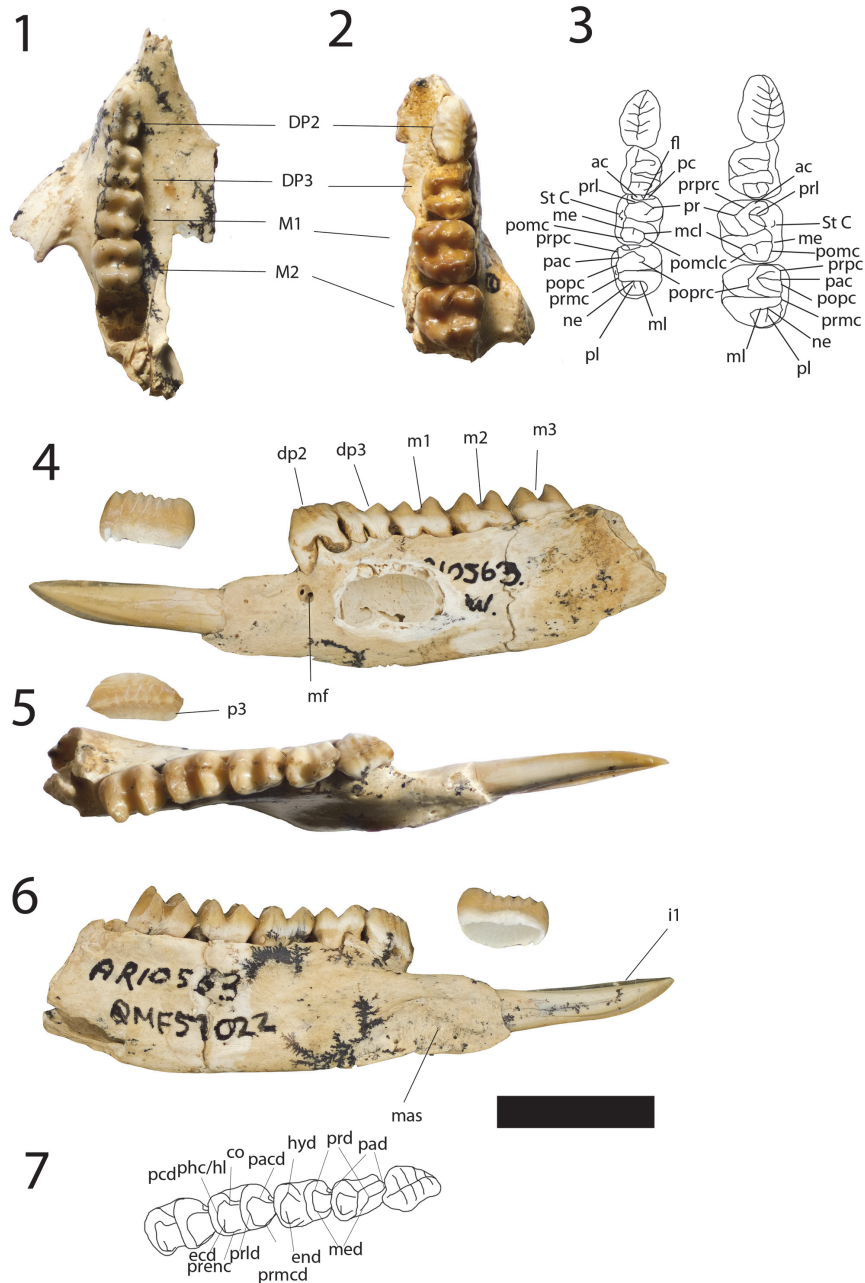
FIGURE 2. Juvenile maxilla of *Ganguroo bilamina* (QM F57020) in occlusal view (**1**), juvenile maxilla of *Bulungamaya delicata/'Nowidgee matrix'* (QM F57024) in occlusal view (**2**), line drawing of upper cheek teeth of *Ganguroo bilamina,* QM F57020, (left), and *Bulungamaya delicata/'Nowidgee matrix',* QM F57024 (right), (**3**) and juvenile dentary of *Ganguroo bilamina* (QM F57022) in buccal (**4**), occlusal (**5**), lingual (**6**) views and line drawing of lower cheek teeth (**7**). **Abbreviations**: **ac**, anterior cingulum; **co**, cristid obliqua; **dP2-3**, deciduous upper premolar two to three; **dp2-3**, deciduous lower premolar two to three; **ecd**, buccal crest from entoconid; **end**, entoconid; **fl**, forelink; **hl**, hypolophid; **hyd**, hypoconid; **i1**, lower first incisor; **m1-m3**, lower molar one to molar three; **M1-M2**, upper molar one to molar two; **mas**, mandibular symphysis; **mcl**, metaconule; **me**, metacone; **med**, metaconid; **mf,** mental foramen; **ml**, metaloph; **ne**, neometaconule; **p3**, lower third premolar; **pac**, paracone; **pacd**, paracristid; **pad**, paraconid; **pc**, precingulum; **pcd**, precingulid; **phc**, posthypocristid; **pl**, postlink; **pomc**, postmetacrista; **pomclc**, postmetaconulecrista; **popc**, postparacrista; **poprc**, postprotocrista; **pr**, protocone; **prenc**, preentocristid; **prd**, protoconid; **prl**, protoloph; **prld**, protolophid; **prmc**, premetacrista; **prmcd**, premetacristid; **prpc**, preparacrista; **prprc**, preprotocrista; **St C**, stylar cusp C. Scale bar equals 10 mm.
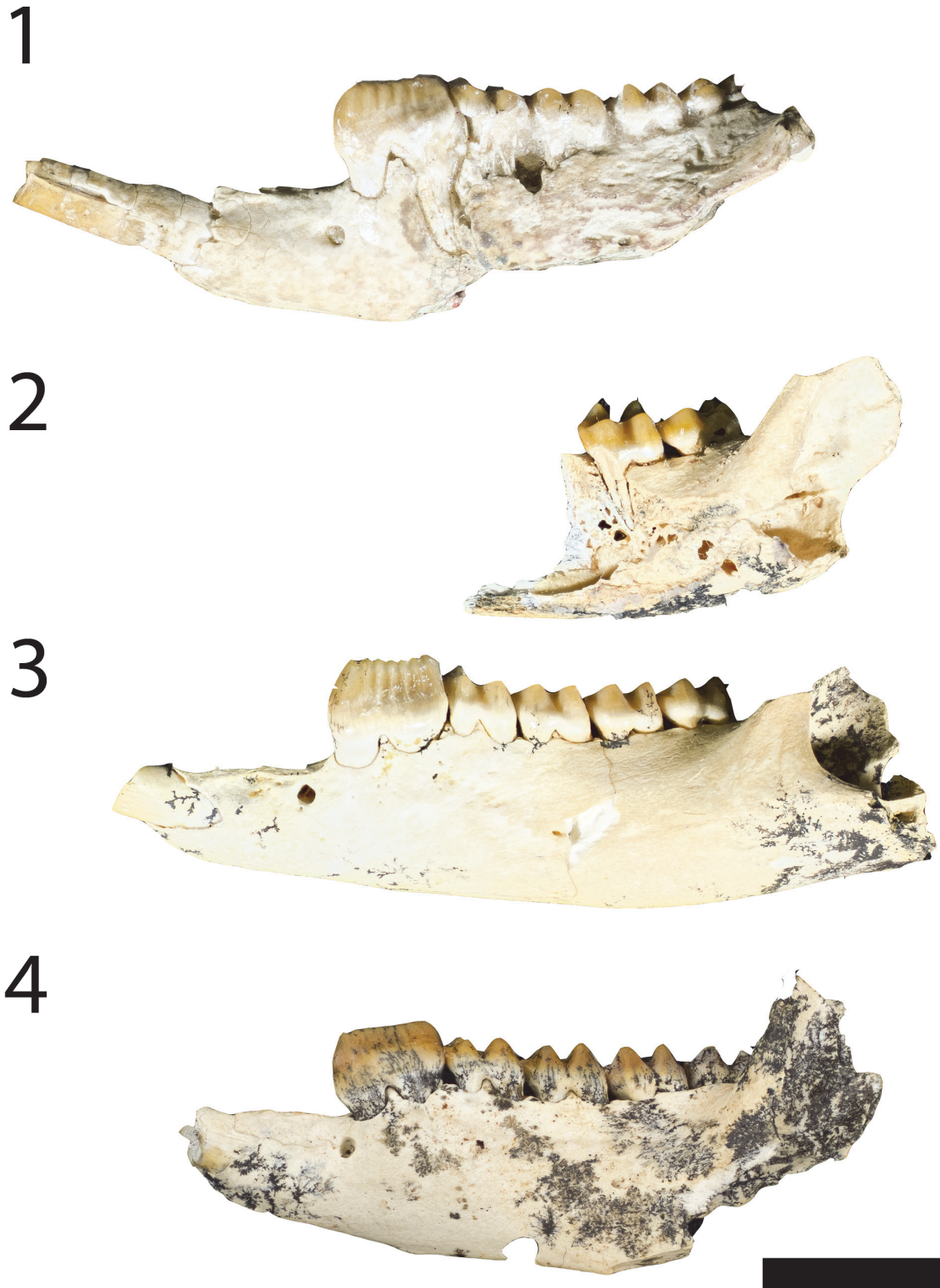
FIGURE 3. Lingual view of dentaries of: **1**, *Bulungamaya delicata* (holotype, CPC 22187) from G Site; **2**, '*Nowidgee matrix*' (QM F19991) from White Hunter Site; **3**, '*Nowidgee matrix*' (QM F19937) from Wayne's Wok Site; and **4,** *Ganguroo bilamina* (QM F57021) from Wayne's Wok Site (reversed for convenience of comparison). Scale bar equals 10 mm.
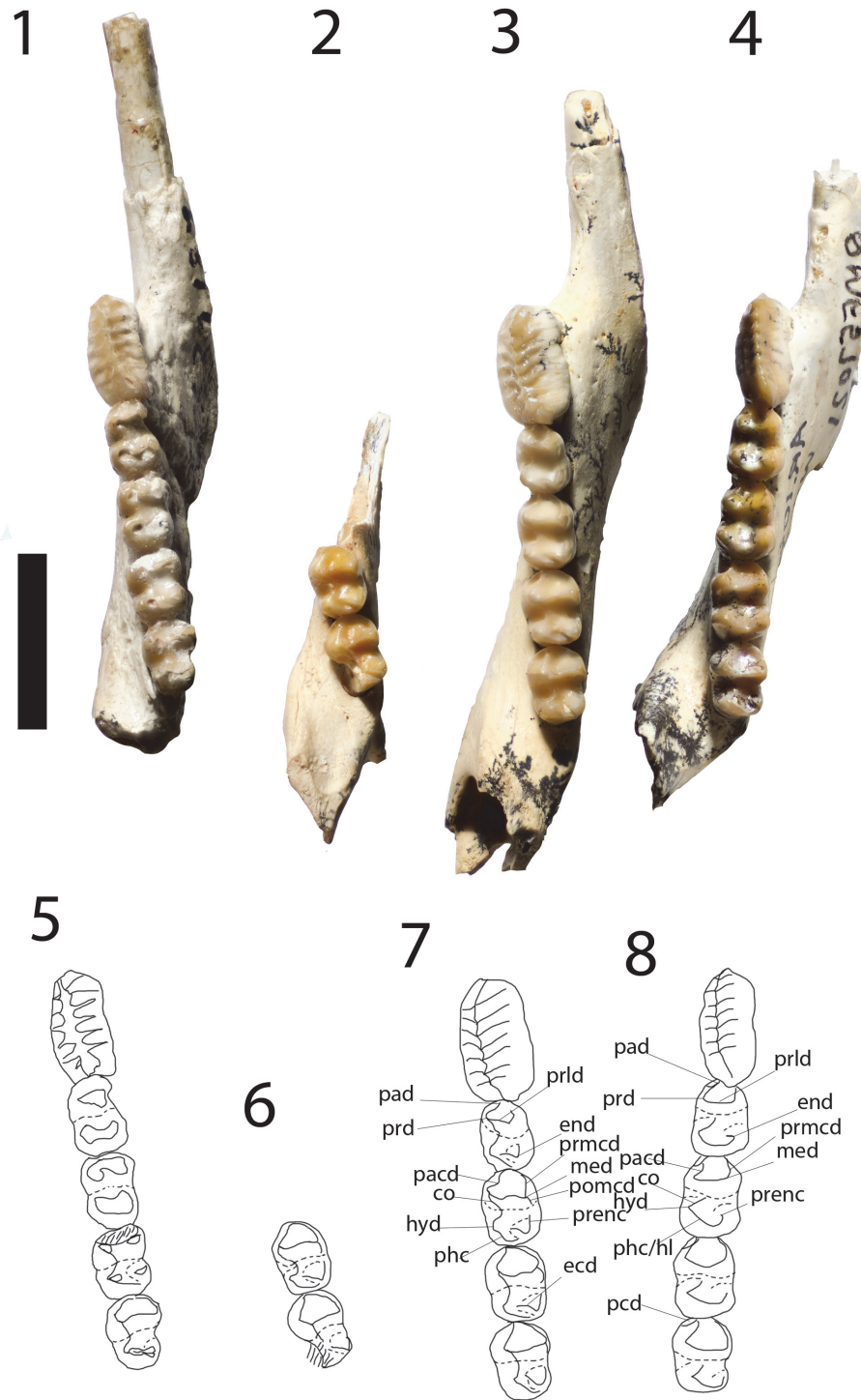
FIGURE 4. Occlusal view of dentaries of and associated line drawings: **1** and **5**, *Bulungamaya delicata* (holotype, CPC 22187) from G Site; **2** and **6**, '*Nowidgee matrix*' (QM F19991) from White Hunter Site; **3** and **7**, '*Nowidgee matrix*' (QM F19937) from Wayne's Work Site; and **4** and **8**, *Ganguroo bilamina* (QM F57021) from Wayne's Work Site (reversed for convenience of comparison). **Abbreviations**: **co**, cristid obliqua; **ecd**, buccal crest from entoconid; **end**, entoconid; **hl**, hypolophid; **hyd**, hypoconid; **mcl**, metaconule; **med**, metaconid; **pacd**, paracristid; **pad**, paraconid; **pcd**, precingulid; **phc**, posthypocristid; **pomcd**, postmetacristid; **prenc**, preentocristid; **prd**, protoconid; **prld**, protolophid; **prmcd**, premetacristid. Scale bar equals 10 mm.

with broken m2, m3, QM F19987, left maxilla with M1-3, QM F23202, left maxilla with M1-4; Ross Scott-Orr (RSO) Site: QM F20039, right dentary with m2-3, QM F20269, right maxilla with M1, broken M2; Upper Site: QM F30396, left dentary with i1, p3, m1-3, QM F19642, left dentary with p3, m1, QM F30397, right dentary with m1-4, QM F20293, right dentary with m2-4, QM F56999, right dentary with dp2-3, p3, m1-2, QM F20271, right dentary with m4, QM F19643, left dentary with damaged m1-4, QM F20295, right dentary with broken m1, m2-3, QM F19947, right dentary with dp2-3, p3, m1, QM F56991, left dentary with dp2-3, p3, m1-2, QM F20272, left dentary with m3, m4 in crypt, QM F19640, left dentary with dp2-3, p3, m1, QM F19646, right dentary with m3, QM F19688, left dentary with i1, dp2-3, m1-3, QM F56993, left maxilla with P3, M1-4, QM F19801, posterior half of a skull, QM F19673, left maxilla with dP3, M1-3, M4 in crypt, QM F56992, right maxilla with P3, M1-3, QM F19985, right maxilla with M1, QM F19885, right maxilla with P3, M1-3, QM F19687, right maxilla with dP2, M1-4, QM F19651, right maxilla with P3, M1, QM F19689, right maxilla with M1-4, QM F19629, right maxilla with dP2-3, M1, QM F19674, left maxilla with P3, M1-4; Wayne's Wok Site: QM F19814, right dentary with p3, m1-2, QM F30399, right dentary with p3, m1-4, QM F19591, left dentary with m3, m4 in crypt, QM F19810, left dentary with m1-4, QM F19835, left dentary with dp2-3, p3, m1, QM F57022, left dentary with i1, dp2-3, p3, m1-3, QM F19836, left dentary with i1, QM F57021, right dentary with i1, p3, m1-4, QM F56998, left dentary with i1, m1-4, QM F19834, right dentary with p3, m1-2, QM F19827, left dentary with broken m1, very worn m2-4, QM F20082, left dentary with m4, QM F19597, left dentary with p3, m1-4, QM F24480, right dentary with m1-2, QM F56997, left dentary with p3, m1-2, QM F20108, left dentary with dp3, p3, m1, QM F20109, right dentary with p3, QM F19602, left dentary with m1-3, QM F50519, left dentary with i1, p3, m1-4, and associated right dentary with p3, m1-4, QM F24050, left dentary with i1, p3, m1-3, QM F30721, left dentary with p3, m1-2, broken m3, QM F20081, right dentary with i1, p3, m1-4, QM F36364, right dentary with i1, dp2-3, m1-2, QM F24477, left dentary with m4, QM F30398, right dentary with p3, m1-4, QM F56257, left dentary with p3, m1-4, QM F24482, left dentary with m2-3, QM F31405, left dentary with p3, m1-4, QM F56260, left dentary with m1-4, QM F36363, right dentary with m3-4, QM F36470, left dentary with broken p3, m1-4, QM F56264, right dentary with p3, m1-3, QM F52814, Skull with left M3-4, right P3, M1-4, QM F57020, associated left and right maxilla with dP2-3, M1-2, QM F20261, left maxilla with dP2-3, P3, M1-3, QM F19589, left maxilla with M1-4, QM F19617, right maxilla with P3, M1-2, QM F19590, left maxilla with P3, M1-4, QM F24219, right maxilla with dP3, P3, M1-3, QM F20163, left maxilla with M1-3, QM F56256, right maxilla with dP3, M1-3, QM F56258, right maxilla with P3, M1-4, QM F56265, Skull with left I1, and left and right I3, P3, M1-4, QM F24475, right maxilla with M1-2, QM F24476, right maxilla with dP3, M1-2, QM F50518, right maxilla with M3-4, QM F56261, right maxilla with M1-2, QM F56255, skull with left and right P3, M1-4, QM F24216, left maxilla with dP2-3, M1-2, QM F56263, right maxilla with P3, M1-2; Kutjamarpu Local Fauna, Leaf Locality, Wipajiri Formation: UCMP 88221, right dentary with i1, p3, m1-4.

Age and Distribution. The holotype is from Wayne's Wok Site, D-Site Plateau, Riversleigh World Heritage Area, northwestern Queensland, Australia (18°15'35"S, 138°06' 41"E). Paratypes and referred specimens are from Riversleigh's Cadbury's Kingdom Site, Camel Sputum Site, Inabeyance Site, Judith's Horizontalis Site, Mike's Menagerie Site, Mike's Potato Patch Site, Neville's Garden Site, RSO Site, Upper Site, Wayne's Wok Site, and the Leaf Locality in the Wipajiri Formation, Lake Ngapakaldi, South Australia. All the Riversleigh site LFs are interpreted to be part of Riversleigh's Faunal Zone B as distinguished by Archer et al. (1989, 1997), Arena (2004) and Travouillon et al. (2006, 2011), except Cadbury's Kingdom LF which is thought to be part of Faunal Zone C, but see discussion below. They are interpreted to be early Miocene in age on the basis of biocorrelation of their contained faunas (Travouillon et al., 2006, 2011). The Leaf Locality (Kutjamarpu Local Fauna) is also interpreted to be early to middle Miocene in age (Megirian et al., 2010; Metzger and Retallack, 2010).

Remarks. The original description of *Ganguroo bilamina* was based on dentaries and lower dentition only. Additional specimens are described below, including a near complete skull, the complete upper dentition and a juvenile upper and lower dentition. Isolated postcranial elements from AL90 Site referred to *G. bilamina* by Kear et al. (2001a) have since been found associated with a skull and dentaries referable to *Ganguroo* sp. 2 rather than *G. bilamina*.

Description

Nasal. Anteriorly, the nasals are level with the anterior part of the premaxilla (Figure 1). The nasal sutures are almost parallel anteriorly but widen posteriorly in the premolar region. The widest part of the nasals occurs above the most anterior part of the lacrimal. The dorsal surface of the rostrum is ventrally curves. The nasal-premaxillary suture is short, half the length of the nasal-maxillary suture. The nares are wider than tall.

Premaxilla. The premaxilla is taller than it is long (Figure 1). The most posterior part of the postero-dorsal process of the premaxilla is a thin flange that posteriorly contacts both the nasal and the maxilla. From this point, the maxillary-premaxillary suture is almost vertical, and ends ventrally at the canine alveolus, which is bordered anteriorly by the premaxilla and posteriorly by the maxilla. The canine is not preserved but the alveolus is considerably larger than the incisive alveoli. Anterior to the canine alveolus, three incisive alveoli are present (with I1 preserved on the left side, and I3 on both sides). The alveolus for I3 is ventrally directed, while the alveoli for I1 and I2 are antero-ventrally directed. The alveolus for I1 is almost three times the size of the alveoli for I2 and I3. Two thin incisive fenestrae are present in the ventral plate of the premaxilla. The most anterior part of the incisive fenestrae is level with the posterior end of the alveolus for I2. The posterior end of the incisive fenestrae is bordered by the maxilla.

Maxilla and Palatine. The maxillopalatine fenestrae are broad, boarded anteriorly by the maxilla and by the palatine laterally at the level of the midpoint of M2, and posteriorly to that point (Figure 1). The maxillofrontal suture is almost horizontal, crossing the facial region just superior to the level of the superior lacrimal foramen. The infraorbital foramen is vertically elliptical, anteriorly directed and located well anterior to the orbital margin above the anterior end of P3. There is little development of the masseteric process of the maxilla, which barely reaches as far ventrally as the alveolar margin which is a normal condition for potoroines (Kear and Cooke, 2001). The suborbital shelf of the maxilla is relatively flat dorsally, broader anteriorly, tapering posteriorly and terminating just posterior to the anterior end of the sphenorbital fissure. Small foramina for the passage of the superior alveoli nerves and vessels open within narrow sulci on the lateral margin of the suborbital shelf. There is a deep infraorbital fossa within the anterior lateral corner of the suborbital shelf and a smaller, more shallow fossa medial to this and superior to the maxillary foramen. The circular opening of this foramen is overhung dorsally by a shelf posterior to the smaller of the two infraorbital fossae and the margin of the shelf continues as a ridge extending horizontally across a dorsal wing of the maxilla, through the maxilla-palatine suture and extending onto the palatine dorsal and posterior to the sphenopalatine foramen located posterior to the maxillary foramen. The sphenopalatine foramen is only just larger than the maxillary foramen and oval in shape. The palatine forms the ventral mesial wall of the orbit.

Lacrimal. The lacrimal extends anteriorly onto the facial region and dorsally beyond the maxillofrontal suture (Figure 1). There is a large inferior lacrimal foramen on the facial region, a superior foramen opening posteriorly on the anterior orbital margin just dorsal to a small prominence. The broad orbital wing of the lacrimal forms the anterior mesial wall of the orbit.

Frontal, Parietal and Interparietal. Anteriorly, the overlapping joint between the frontal and the nasal crosses transversely from the anterior of the maxillofrontal suture to the frontal/frontal suture (Figure 1). The frontal region is broad in the interorbital region, contrasting markedly with the constriction of this region seen in balbarines, and is remarkably flat. Strong supraorbital crests on the lateral margins of the flat dorsal portion of the frontals continue posteriorly along the lateral, dorsal margin of the parietal as sagittal crests, converging on the midline on the posterior dorsal surface of the neurocranium. Here they form a single sagittal crest that continues posteriorly through the overlapping interparietal sutures. The interparietal and supraoccipital sutures form a tall crest that ends at the junction of the parietals and the supraoccipital. The rostrum is very broad anterior to the orbital region but does not exhibit the marked inflation seen in this region in balbarines (Cooke, 2000; Kear et al., 2007). The parietals are laterally flared at their posterior ends and curve gently dorsally, indicating a well-developed nuchal crest. There is a clear, broad contact between the alisphenoid and parietal on the lateral wall of the neurocranium. While short parietal-alisphenoid contact is known to occur among Riversleigh macropodoids, e.g., in *Hypsiprymnodon bartholomaii* (Flannery and Archer, 1987a) and *Bettongia moyesii* (Flannery and Archer, 1987b), the condition seen here is much more extensive and far more resembles that seen in macropodoids rather than that in potoroines and hypsiprymnodontids (Kear and Cooke, 2001).

Zygomatic arch. The jugal ends anteriorly at the level of the anterior margin of the lacrimal (Figure 1). Its lateral surface has a crest arising anterior to the masseteric process and running posteriorly below the orbit to the posterior end of the jugal. The crest marks the anterior and dorsal limit of attachment of the superficial layer of the masseter. The orbital part of the jugal is overhung anteriorly by the ventral margin of the orbit. The zygomatic arch makes a smooth transition to the facial region, there being no antorbital sulcus, absence of this feature being the condition in potoroines. The most anterior part of the jugal-squamosal suture is V-shaped, with the jugal extending dorsally as well as dorsoventrally. The posterior end of the jugal ventrally overlaps the zygomatic process of the squamosal and forms the anterior margin of the glenoid fossa. The zygomatic process of the squamosal is wide transversely at its posterior end, surmounted by a broad, shallow sulcus. The process is relatively shallow and has a flat lateral surface. The glenoid fossa is broad and flat and merges smoothly with the ventral surface of the zygomatic process, which projects anteriorly for a considerable distance. There is a well-developed pneumatised postglenoid process posterior to the glenoid fossa.

Neurocranium. The parietals form most of the roof and walls of the neurocranium, having a broad lateral contact with the squamosals (concave in shape) which form the posteroventral lateral walls (Figure 1). The anteroventral component of the neurocranial wall is contributed by the temporal wing of the alisphenoid. The anteriorly facing foramen rotundum is visible at the anteroventral margin of the temporal wing of the alisphenoid, lateral to the sphenorbital fissure (foramen rotundum is better preserved in QM F19801). Retained suture lines between parietals and the supraoccipital indicate that the later contributed significantly to the posterior roof of the neurocranium.

Basicranium. The basioccipital is roughly hexagonal in outline with a relatively broad anterior contact with the basisphenoid (Figure 1). Paired foramina lie within fossae overhung by the ventral margin of each of the occipital condyles. Very short canals leading from these foramina open posteriorly within the foramen magnum. The most anterior of these foramina opening on the ventral surface of the basioccipital are presumed to represent the hypoglossal foramina, the more posterior foramina being the condylar foramina. The jugular foramina lie lateral to the condylar foramina, posterior to the alisphenoid tympanic wing and mesial to the ante-

rior ends of the paracondylar process of the exoccipital. The foramina for the greater petrosal nerves are mesial to the alisphenoid tympanic wing, posteromesial to the secondary foramina ovale and closely posterolateral to the carotid foramina. The alisphenoid tympanic wings are relatively flat and poorly inflated and terminate posteriorly at the base of the short, laterally compressed paracondylar process of the exoccipital. The secondary foramen ovale opens on the anteromesial side of the alisphenoid tympanic wing and is floored by a thin, very narrow process of the alisphenoid tympanic wing that separates it from the foramen for the greater petrosal nerve which lies posteroventral to the secondary foramen ovale. Contribution of a ventral floor to the secondary foramen ovale by a process of the alisphenoid was regarded by Murray (1991) to be typical of macropodoids, contrasting with the incomplete ventral floor provided for the secondary foramen ovale by the process of the alisphenoid which is the usual condition in potoroines. The carotid foramen is anterior to the posterior margin of the basisphenoid in QM F56265 and QM F19801, but more posteriorly located and lateral to the basisphenoid-basioccipital suture in QMF 52814. Murray (1991) suggested that an anterior position for the carotid foramen was a potoroine synapomorphy. The transverse foramen of the basisphenoid in QM F56265 and QM F19801 is single with a shallow sulcus, presumably for the Eustachian tube where it crosses the ventral border. In QMF 52814, the transverse foramen is incompletely divided by dorsal and ventral spurs, and there is no sulcus ventral to it.

The pterygoid fossae are oval in outline with ventrolaterally sloping mesial walls provided by the pterygoid and an anterior wall provided by the alisphenoid. The internal surfaces of the pterygoid fossa are relatively smooth.

The posterior vertical face of the occipital does not exhibit obvious muscle attachment scars for the neck musculature. The foramen magnum is teardrop-shaped. The width of the posterior surface of the skull is extended by the vertically elongate mastoids.

Auditory Region. The ectotympanic is roughly square in ventral outline and concave in its central region (Figure 1). The external auditory meatus is not enclosed dorsally by the ectotympanic but is closed by a thin plate of the squamosal. The small stylo-mastoid foramen is located immediately anterior to the ectotympanic/mastoid suture. The mastoid process is relatively long, more massive than

the paracondylar process of the exoccipital and inclined ventrolaterally.

The articular eminence of the glenoid fossa is roughly square. The postglenoid foramen is mesial to the low triangular postglenoid process and is partially divided by a spur of the ectotympanic from the smaller and more mesial residual Gasserian fissure. A large opening into the epitympanic sinus posterior to the postglenoid process represents the zygomatic epitympanic sinus of the squamosal which is enclosed entirely by the squamosal.

The lateral wall of the petrosal is visible through the suprameatal foramen, on the posterior lateral wall of the squamosal, dorsal to the exit of the auditory meatus. The dorsal opening of the temporal canal lies within this opening, anterior to the visible portion of the petrosal. The cerebellar face of the petrosal (visible in QM F19801) more closely resembles that of *Macropus* than *Potorous* or *Hadronomas* in so far as these are illustrated by Murray (1991). The parafloccular fossa is deep, undercutting the edges of the orifice. The endolymphatic duct opens on the cerebellar face of the petrosal, as it does in *M. robustus* (Murray, 1989).

Upper Dentition. The description which follows is based primarily on the upper dentition preserved in the skull (Figure 1), with variation evident in other specimens noted where appropriate.

The chisel-like I1 is the largest upper incisor. It has an oval occlusal outline but in buccal view it is strongly anteriorly curved. Its alveolus is anteroventrally orientated. The I2 is absent in QM F56265 but its anteroventrally-orientated alveolus is small, circular in shape and more ventrally situated than the alveolus of I1. The I3 is oval in occlusal outline with a central bladed crown. It would have been larger than I2 but it is smaller than I1. While its alveolus faces ventrally, the crown of I3 is anteroventrally orientated.

In occlusal view both cheek teeth rows are slightly buccally convex. The long axes of the premolars are aligned with the molar row. In lateral view the posterior molars are more ventrally situated than the anterior molars and the occlusal margins of the premolars project beyond those of the adjacent molars. Molars are low-crowned, bilophodont and larger in the middle of the row than at its ends.

dP2 is preserved in QM F19857, F19861, F19976 and in both tooth rows of F57020 (Figure 2). The tooth is short, blade-like and slightly longer than dP3. The occlusal margin is subhorizontal and shorter than the crown base. It begins posterior to the anterior margin of the crown base and extends to the level of the posterior margin of the tooth. The lingual face of the crown is steeper than the buccal face. Three minor cuspules anterior to a longer cusp are present on the occlusal crest and all four cuspules support transcristae. Some lingual portions of these transcristae are obscured by wear in some specimens. A strong posterior crest runs from the apex of the posterior cuspule and sweeps lingually as it approaches the crown base. In QM F57020, an additional posterior, lingual transcrita runs parallel to and just anterior to this posterior crista.

dP3 is preserved in QM F56995, F19857, F19861, F19976, F57020 and F20261 (Figure 2). The tooth has a straight buccal margin and a convex lingual margin which may be constricted at the level of the interloph. The occlusal surface is dominated by a longitudinal ridge continuing the line of the occlusal blade of dP2 and formed by the prominent, laterally compressed parastyle, similarly compressed paracone and metacone and their associated pre- and postcristae. The postparacrista and premetacrista form a continuous centrocrista that is interrupted by a narrow interloph cleft in QM F57020. This tooth is bilophodont, with a poorly developed protoloph and metaloph. A neometaconule and associated crest (postlink) are present at the midpoint of the metaloph.

P3 is a long and relatively low blade-like tooth with an occlusal edge that is horizontal over most of its length but has a taller buccally-orientated posterior 'heel' (Figure 1). In occlusal view the crown base has a sub-elliptical outline but is slightly constricted just anterior to the posterior 'heel'. There is a very well-developed lingual ridge buttressing the posterior end of the occlusal blade. A shelf-like lingual cingulum extends from the anterior margin to the posterior lingual ridge, and the expanded buccal crown base forms a relatively rounded buccal cingulum. There are six cuspules on the occlusal margin anterior to the posterior 'heel', each having associated transcristae that extend to the crown base. The number of cuspules varies in other specimens from five to as many as seven (e.g., in QM F20253). The variation in the number of cuspules and transcristae is caused by dental wear. A crest extends anteriorly from the apex of the most anterior cuspule to the crown base. A better developed but shorter crest is associated with the posterior surface of the posterior 'heel'.

M1 is almost square in occlusal outline, the protoloph and metaloph being subequal in length (Figure 1). Lingual cusps are more massive and

have more rounded apices than those of the buccal side. The buccal surfaces of the crown slope more steeply than the lingual surfaces. The short preparacrista slopes very slightly lingually from the apex of the paracone to the anterior margin of the crown. The protoloph is formed by a lingually sloping crest from the paracone which meets an anterolingually-inclined preprotocrista at a low point on the approximate midline of the loph. The preprotocrista continues anteriorly as a 'forelink', although its prominence has been reduced by wear. An anterior cingulum extends across the buccal anterior margin from the preparacrista to the 'forelink', and a precingulum extends from there to the lingual margin. The postparacrista slopes directly posteriorly from the paracone apex to the interloph valley where it is linked to the curved premetacrista thereby forming a continuous centrocrista. A short ridge on the posterobuccal flank of the paracone connects to a distinct stylar cusp C which occupies the anterior half of the buccal end of the interloph valley. Stylar cusp D is not developed but a stylar crest on the anterior buccal face of the metacone links the premetacrista to the base of StC. Stylar cusp C is reduced in size in some specimens, and the crest representing StD similarly reduced. The postprotocrista slopes posterobuccally to the interloph valley and extends almost to the occlusal margin of the metaloph, meeting it just buccal to the metaconule. There is a distinct prominence, the neometaconule, along the midline of the crest of the metaloph. A broad, rounded neometaconule crista (the 'postlink') extends from this neometaconule onto the posterior face of the metaloph. The postmetacrista extends from the apex of the metacone to the crown base where it meets the postmetaconulecrista which sweeps across the posterior face of the loph.

M2 is similar in shape to M1 except in the following features (Figure 1): it is larger than M1 and wider anteriorly than posteriorly; stylar cusp C is not as large; the postparacrista and premetacrista are flexed lingually in the interloph valley; and stylar crest D is not as well developed.

M3 is similar in shape to M2 except in the following features (Figure 1): it is narrower posteriorly; stylar cusp C is reduced to a stylar crest (absent in some specimens); the postparacrista and premetacrista sometimes fail to meet in the interloph region; and the neometaconule and its cristae are not as well developed.

M4 is similar in shape to M3 except in the following features (Figure 1): it is considerably narrower posteriorly; its metaloph is narrower than its

protoloph; and both stylar crests are absent from the interloph valley.

Lower Dentition. The lower dentition is described by Cooke (1997a). However, one of the specimens used in that description as dp2 and dp3 (QM F23777) have been referred here to *G. bites*. Further, QM F19385 is a worn and damaged specimen of *G. bilamina*. Additional juveniles of *G. bilamina* have since been recovered (e.g., QM F57022, QM F56996, F20248, F20019, F19903, F56254, F24744, F20006, F56999, F19947, etc.). The morphology of these specimens is consistent with the descriptions of the taxa provided by Cooke (1997a) except as follow (Figures 2, 3, 4): a buccal crest from the entoconid is present on dp3 and all lower molars (decreasing in development posteriorly) in some juvenile (e.g., QM F57022, F56996, F20019, F56991) but absent in others (e.g., QM F19640, F19947, F20108). This buccal crest is absent in all adult specimens, possibly due to wear. Unworn p3 reveal a total of seven cuspids and associated transcritids, instead of six described by Cooke (1997a). Wear tends to occur posteriorly, wearing down the seventh cuspid and transcristid first, then the sixth and so on.

Ganguroo bites, n. sp.
Figure 5

Species Diagnosis. *Ganguroo bites* differs from *G. bilamina* in the following features: it has eight cuspids and associated transcristids on p3 (instead of 7 in *G. bilamina*); a longer but much narrower p3; larger and much wider molars that are almost square in occlusal outline; a paraconid present as a small cusp in m2-3; and no buccal crest from the entoconid.

Species etymology. Named after the Riversleigh fossil locality, Bitesantennary Site.

Holotype. QM F23776, left dentary with p3, m1-3.

Paratypes. QM F23775, right dentary with m1-2, m3 in crypt; QM F23777, juvenile left dentary with dp2-3, m1.

Age and Distribution. The holotype and paratypes are from Bitesantennary Site, D-Site Plateau, Riversleigh WHA, northwestern Queensland. Bitesantennary LF is interpreted to be part of Riversleigh's Faunal Zone B as distinguished by Archer et al. (1989, 1997), Arena (2004) and Travouillon et al. (2006, 2011). It is interpreted to be early Miocene on the basis of biocorrelation of its contained faunas (Travouillon et al., 2006, 2011).

Remarks. QM F23777 was originally listed as a paratype of *Ganguroo bilamina.* In light of addi-
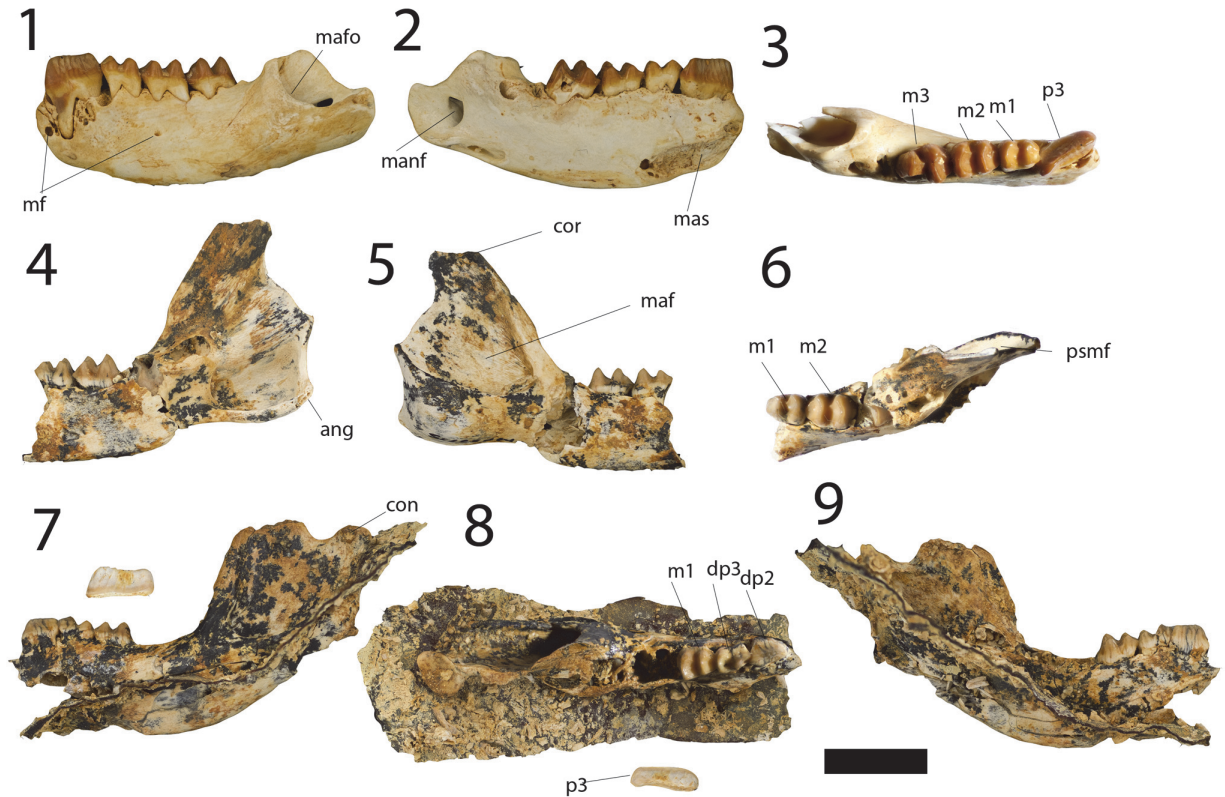
FIGURE 5. *Ganguroo bites* n. sp., holotype QM F23776, from the Bitesantennary Site, left dentary in lingual (**1**), buccal (**2**) and occlusal (**3**) views; Paratype QM F23775, right dentary in buccal (**4**), lingual (**5**) and occlusal (**6**) views; and Paratype QM F23777, left dentary in buccal (**7**), occlusal (**8**) and lingual (**9**) views. **Abbreviations**: **ang**, angular process; **dp2-3**, deciduous lower premolar two to three; **i1**, lower first incisor; **m1-m3**, lower molar one to molar three; **maf**, masseteric fossa; **mafo**, masseteric foramen; **manf**, mandibular foramen; **mas**, mandibular symphysis; **mf,** mental foramen; **p3**, lower third premolar; **psmf**, posterior shelf of the masseteric fossa. Scale bar equals 10 mm.

tional material found in the Bitesantennary Site, this specimen and others from the same site exhibit morphological features that clearly distinguish it from that species.

Description

The holotype is a left dentary with p3 to m3 and alveoli for m4 (Figure 5). The dentary is incomplete anterior to p3. The ventral margin of the horizontal ramus is convex and deepest below the roots of m2. No distinct digastric prominence is present. Two mental foramina are present on the buccal margin of the dentary, one larger foramen just anterior to p3, and one smaller foramen below the anterior root of m2.The ascending ramus is not preserved in the holotype but it is almost completely preserved in QM F23775 and partly preserved in QM F23777. The angle formed by the occlusal margin and the ascending ramus is about 120 degrees. The masseteric foramen is large and deep, extending at least below the anterior region of m3. Posteriorly, the masseteric foramen is confluent as a large oval opening with the mandibular foramen in the holotype, but is confluent as a small oval opening with the mandibular foramen in QM F23775 and QM F23777. This difference may be linked to age; QM F23775 and QM F23777 are juveniles while the holotype is an adult. The condyle, present in QM F23777, is broad and elliptical in dorsal view.

The dp2 and dp3 are preserved in QM F23777 (Figure 5). The dp2 crown is plagiaulacoid in form and slightly longer but narrower than m1. The occlusal margin is shorter than the crown base. The buccal face of the crown is less steep than the lingual face. Four cuspids are present anterior to a much larger posteriorly positioned cuspid. Transcristids are associated with the four anterior cuspids only.

The dp3 is a molariform tooth, shorter but wider than dp2 (Figure 5). It is almost rectangular in shape with the buccal margin concave and the

14

lingual margin convex. The trigonid is laterally compressed. The protoconid is the tallest cusp on the crown, followed by paraconid, entoconid and hypoconid. No distinct metaconid is present. The paracristid is anteroposteriorly orientated, while the metacristid is posterolingually orientated. The entoconid is situated posterolingual to the protocone. No distinct preentocristid is present. The entoconid is joined to the hypoconid laterally by the hypolophid. The cristid obliqua extends from the hypoconid anterolingually and ends in the interlophid valley, posterobuccal to the protoconid.

The p3 is represented in the holotype (QM F23776) and the paratype (QM F23777; Figure 5). In the latter specimen, p3 is erupted but the posterior alveoli for dp2 and dp3 are still visible, and the p3 blade is not aligned with the molar row. This arrangement indicates that the specimen may represent a young adult (the m4 alveoli indicate that it was fully erupted) in which p3 had not yet come into alignment with the molars (dp2 and dp3 are aligned with the molars in QM F23777). The p3 is a long, plagiaulacoid-like tooth, about one and a half times the length of m1, but narrower than the anterior width of m1. The p3 width is greater anteriorly than posteriorly. Eight cuspids are present along the occlusal edge of the tooth. The seven smaller anterior cuspids have associated transcristids but the large posterior cuspid does not.

The m1 is subrectangular in occlusal outline, but wider posteriorly than anteriorly (Figure 5). The hypoconid is the tallest cuspid, followed by the entoconid, metaconid and protoconid in decreasing height. The m1 is bilophodont. The protoconid is connected to the metaconid lingually by a nearly straight protolophid. A short premetacristid extends anteriorly to the anterior margin of the tooth. The paracristid extends from the protoconid anterolingually to join the premetacristid anteriorly thereby enclosing a broad anterior cingulum. No distinct paraconid is present. A small precingulid is present on the anterobuccal flank of the paracristid. The entoconid is directly posterior to the metaconid and is joined to the hypoconid by a concave hypolophid. A preentocristid extends anteriorly from the entoconid and terminates in the interlophid valley directly posterior to metaconid. The cristid obliqua runs from the hypoconid anterolingually and ends in the interlophid valley posterolingual to the protoconid. No posterior cingulid is present.

The m2 is similar in morphology to m1 but differs as follows: it is larger, wider and longer in occlusal outline; the paraconid is present as a distinct cusp on the paracristid, just anterolingual to

the protoconid; the protoconid is the second tallest cuspid (after the hypoconid), followed by the entoconid, metaconid and paraconid; the anterior cingulid and precingulid are wider; the premetacristid is less well-developed; the preentocristid is absent.

The m3 is similar in morphology to m2 but differs as follows: it is larger, wider and longer in occlusal outline; the trigonid is wider than the taloned; the paraconid is taller.

Genus *BULUNGAMAYA* Flannery et al., 1983
Bulungamaya delicata Flannery et al., 1983
Figures 2, 3, 4

v. 1997 *Nowidgee matrix* Cooke, 1997a, p. 282-288, figs. 1-2.

Revised Diagnosis. *Bulungamaya delicata* is characterised by the following features: a buccally expanded masseteric canal; a sharp ventrally convex dentary margin below m1-2; i1 has its enamel confined to the buccal surface where it is extensive; ventral and dorsal flanges are present on i1; p3 and P3 are elongate with seven cups and cuspids (contra Flannery et al., 1983) with associated fine transcritids and transcristae (although coarser than in species of *Ganguroo*) and a bulbous base; a small alveolus for i2 is present directly posterior to i1; lower molars and dp3 are bunolophodont with well-developed posthypocristids, no connection between the entoconid and hypoconid, protoconid connected to cristid obliqua and no posterior cingulid present; m1 lacks a protostylid; m4 is not greatly reduced in size relative to the other molars in contrast to the condition in potoroines and hypsiprymnodontids (Kear and Cooke 2001); dP3 is bilophodont but the upper molars are bunolophodont, having an incomplete the protoloph (no connection between protocone and paracone), but a complete metaloph (the metacone connects to the metaconule); and a large stylar cusp C on all upper molars.

Bulungamaya delicata differs from species of *Ganguroo, Wabularoo* and all macropodines, sthenurines and balbarids in having bunolophodont molars instead of bilophodont (Cooke, 1997a; Archer, 1979; Kear and Cooke, 2001; Prideaux, 2004). It differs from hypsiprymnodontids in having elongate premolars, but differs from all potoroines in having shorter and more bulbous premolars (Kear and Cooke, 2001).

Holotype. CPC22187, left dentary containing partial i1, p3, m1-4.

Referred Material. Camel Sputum Site: QM F30390, right dentary with i1, p3, m1-4, QM F19961, left dentary with m1-4, QM F20255, right dentary with m3-4, QM F22761, left dentary with

m1-2, QM F30392, right dentary with dp3, p3, m1-2, QM F30394, right dentary with p3, m1-4, QM F30395, right maxilla with P3, M1-4, QM F19962, right dentary with m4, QM F19984, left dentary with m1, QM F19974, right dentary with m1-2, QM F30723, right dentary with m1-3, QM F57023, left maxilla with P3, M1-4, QM F19965, right maxilla with P3, M1-2, half of M3, QM F19954, left maxilla with M2-4, QM F19953, left maxilla with dP3, M1-2, QM F23491, right maxilla with M1-3, QM F20285, left maxilla with dP3, M1-2, QM F19675, right maxilla with P3, M1-2, QM F20310, right maxilla with M2-4; D -Site: QM F10650, right dentary containing the root of i1; Dirk's Towers Site: QM F24651, left dentary with p3, m1-4, QM F30718, right dentary with p3, m1-4, QM F29702, right maxilla with P3, M1-3; Judy's Jumping Joint Site: QM F57024, left maxilla with dP2-3, M1-2; Keith's Chocky Block Site: QM F57012, right m1; Neville's Garden Site: QM F20011, right maxilla with M1-2; Upper Site: QM F30393, right dentary with dp3, m1, QM F19986, left maxilla with M1-2, QM F19619, right maxilla with P3, M1; Wayne's Wok Site: QM F19937, left dentary with p3, m1-4, QM F20069, left dentary with dp2-3, p3, m1-2, QM F20080, right dentary with dp2-3, p3, m1-3, m4 in crypt, QM F30391, left dentary with m1-2, m3 in crypt, QM F56988, right dentary with i1, p3, m1-4, QM F19579, left dentary with p3, m1-3, QM F24184, left dentary with m2-3, QM F19586, left dentary with dp2, p3, m1-3, m4 in crypt, QM F24191, left dentary with dp2-3, broken p3, m1, QM F20165, right dentary with m1-2, m4 in crypt, QM F56253, left dentary with dp2-3, m1-3, QM F19616, left maxilla with M1-3, QM F19939, left maxilla with M1-4, QM F56989, left maxilla with P3, M1-2, QM F19918, right maxilla with P3, M1-4, QM F30831, left maxilla with M1-4, QM F24478, right maxilla with M2-4; White Hunter Site: QM F19991, left dentary with m3-4.

Age and Distribution. The holotype is from G Site, D Site Plateau, Riversleigh WHA, northwestern Queensland, Australia. The age of G Site is interpreted to be equivalent to the Riversleigh Local Fauna (="D -Site LF"), Riversleigh Faunal Zone A, late Oligocene (Archer et al., 1989, 1997; Arena, 2004; Travouillon et al., 2006, 2011). White Hunter LF is also interpreted to be a part of Riversleigh's Faunal Zone A. Camel Sputum LF, Dirk's Towers LF, Judy's Jumping Joint LF, Upper LF and Wayne's Wok LF are part of Riversleigh's Faunal Zone B, early Miocene in age. Keith's Chocky Block LF is part of Riversleigh's Faunal Zone C, middle Miocene in age.

Remarks. Dental descriptions of *Bulungamaya delicata* are provided by Flannery et al. (1983) and Cooke (1997a). Arguments for subsuming *Nowidgee matrix* into *B. delicata* can be found in the discussion below. Description of the previously unknown upper deciduous premolars follows.

Description

The dP2 and dP3 are preserved in QM F57024 (Figure 2). The dp2 is plagiaulacoid, about as long as M1 but only two thirds the widths. The occlusal margin is relatively horizontal and about one third shorter than the length of the crown base. The lingual face of the crown is steeper than the buccal face. Five cusps are present on the occlusal crest and have transcristae associated with them, although the posterior transcristae are much less obvious than anteriorly.

The dP3 is a molariform tooth (Figure 2), bilophodont and shorter than dP2 and wider (but not as wide as M1). The tooth has a straight buccal margin and a convex lingual margin. The paracone is the tallest cusp on the occlusal surface followed by the metacone, metastyle, parastyle, neometaconule, metaconule and protocone, in decreasing order. A tall preparacrista joins the parastyle at the most anterobuccal corner of the tooth. The postparacrista descends from the paracone posterolingually and meets the premetacrista, forming a complete centrocrista at the buccal end of the interloph valley. The premetacrista joins the metacone posterobuccally. The postmetacrista departs from the metacone posteriorly and joins to a small cusp, possibly the metastyle, before curving posterolingually to meet the postmetaconulecrista at the most posterior edge of the tooth. The postmetaconulecrista continues anterolingually and connects to the metaconule. The metaloph joins the metaconule to the metacone transversely, through a small neometaconule, located about halfway between the metaconule and the metacone. Similarly, the protoloph joins the paracone to the protocone, but this crest is shallow lingually. The postprotocrista departs the protocone posterobuccally and ends in the interloph valley, at the anterior flank of the metaloph, anterobuccal to the metaconule. No anterior cingulum is present; instead, the lingual flank of the preparacrista is wide and steep.

RESULTS

Coefficient of Variation Analysis

Coefficients of variation (CVs) for *Thylogale stigmatica* (Appendix 8) range between 3.54 and 12.5, generally falling within the expected range (4–10) for a single mixed-sex population (Simpson et al., 1960). The second lower molar was the least variable tooth in overall size (CVs 3.54–4.83) while p3 was the most highly variable tooth (CVs 7.6–12.5). P3 was the only other tooth to have values over 10 (CV = 11.35).

Thylogale thetis (Appendix 9) was slightly less variable with CVs ranging between 4.98 and 11.16. The third upper molar was the least variable tooth in overall size (CVs 5.28-5.95), but m1 was the most variable tooth (CVs 9.06-11.16), followed by p3 and P3.

When *Thylogale stigmatica* and *T. thetis* are combined (Appendix 10), the range increases to values between 5.06 and 16.33. The second lower molar (CVs 6.01–6.52) and third upper molar (CVs 5.86–6.19) remained the least variable teeth, and p3 (CVs 11.75–16.33) remained the most variable tooth followed by P3 (CVs 9.71–13.25) and m1 (CVs 7.09–9.09).

CVs ranged between 3.28 and 7.99 for *Ganguroo bilamina* (Appendix 11) and between 2.06 and 8.86 for the combined sample of *Bulungamaya delicata* and '*Nowidgee matrix*' (Appendix 12). In both cases, they followed the trends seen in species of *Thylogale,* with p3 being the most variable tooth followed by P3 and m1, but in the combined sample of *Bulungamaya delicata/'Nowidgee matrix',* m4 and M4 were more variable than m1.

Bivariate Plots

Bivariate plots of dental variables for species of *Thylogale* (Appendices 13, 14, 15, 16) show a strong separation for p3 and P3, except for one specimen overlapping in p3 length versus posterior width. Length of P3/p3 seems to correlate with gender, with one sex having slightly longer premolars than the other, but while males generally have longer premolars in *T. thetis,* they are generally shorter than those of females in *T. stigmatica.*

In contrast, upper and lower molars do not show a clear separation and mostly overlap in their range (Appendices 13, 14, 15, 16). There is no distinct separation of males and females either, except in *Thylogale thetis* m4s which are distinctively larger in males. There is no significant difference between using anterior or posterior width versus length. In upper molars, females of each species greatly overlap. Males overlap much less and tend to occupy opposite spectra (short and wide versus long and narrow). This is also reflected in the overall size of the upper teeth where *T. thetis* has smaller premolars but larger molars than *T. stigmatica.* This pattern does not seem to be present in lower molars.

Bivariate plots of upper dentition of *Ganguroo bilamina* and '*Nowidgee matrix*' are shown in Figure 6. These two species are almost completely separated by P3 measurements except for one specimen of *N. matrix* from Dirk's Towers (QM F29702) which falls well within the range of *G. bilamina.* Upper molar measurements overlap greatly between the two species.

A similar pattern is found in the lower dentition (Figure 7) where very little overlap exists in p3 measurements of *Ganguroo bilamina* and *Nowidgee matrix* but greatly overlap in m1-4. A specimen of *G. bilamina* from the Leaf Locality (Kutjamarpu Local Fauna) falls within the range of Riversleigh specimens for all dental measurements. The holotype of *Bulungamaya delicata* falls within the range of *N. matrix* for all comparable teeth. *Ganguroo bites* does not fall within the range of any other species for p3 and m2. It overlaps with both *G. bilamina* and *N. matrix* in its m1 measurements. *Purtia mosaicus* overlaps with *N. matrix* in its p3 measurements only, while *Ngamaroo archeri* overlaps with *P. mosaicus* and *N. matrix* only in its m1 dimensions.

Principle Components Analysis

In the PCA of the upper dentition (Appendix 17.1), Component 1 accounts for 39.32% of the variance while Component 2 accounts for 27.98% of the variance. Other components accounted for less than 8% of the variance (e.g., Component 3 = 8%, Component 4 = 4.83%, etc.). P3 length and width were the most useful measurements for separation, followed by M4 length, M2 to M4 anterior width and M1 posterior width.

In the PCA of the lower dentition (Appendix 17.2), Component 1 accounts for 44.02% of the variance while Component 2 accounts for 30.84% of the variance (Component 3 = 7.93%, Component 4 = 4.71%, etc.). The p3 length and width were the most useful measurements followed by m1 and m3 lengths.

The PCA of the upper dental variables of *Ganguroo bilamina* and '*Nowidgee matrix*' (Figure 8) shows significant overlap. Component 1 accounts for 27.36% of the variance while Component 2 accounts for 14.97% of the variance (Component 3
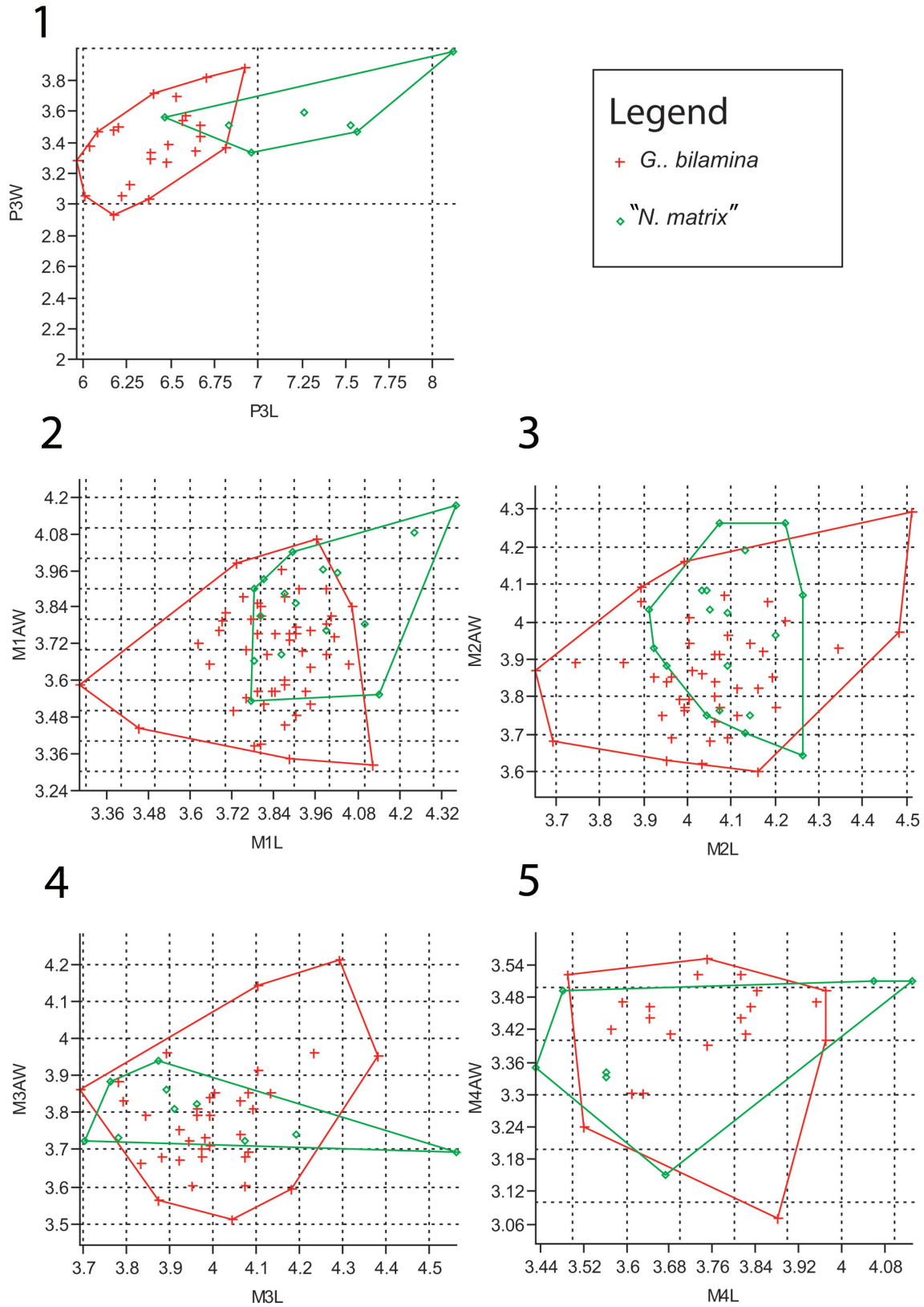
FIGURE 6. Bivariate plots of upper dentition of *Ganguroo bilamina* and '*Nowidgee matrix'.* L – anteroposterior length, AW = anterior width, W = maximum width, P = premolar, M = molar.
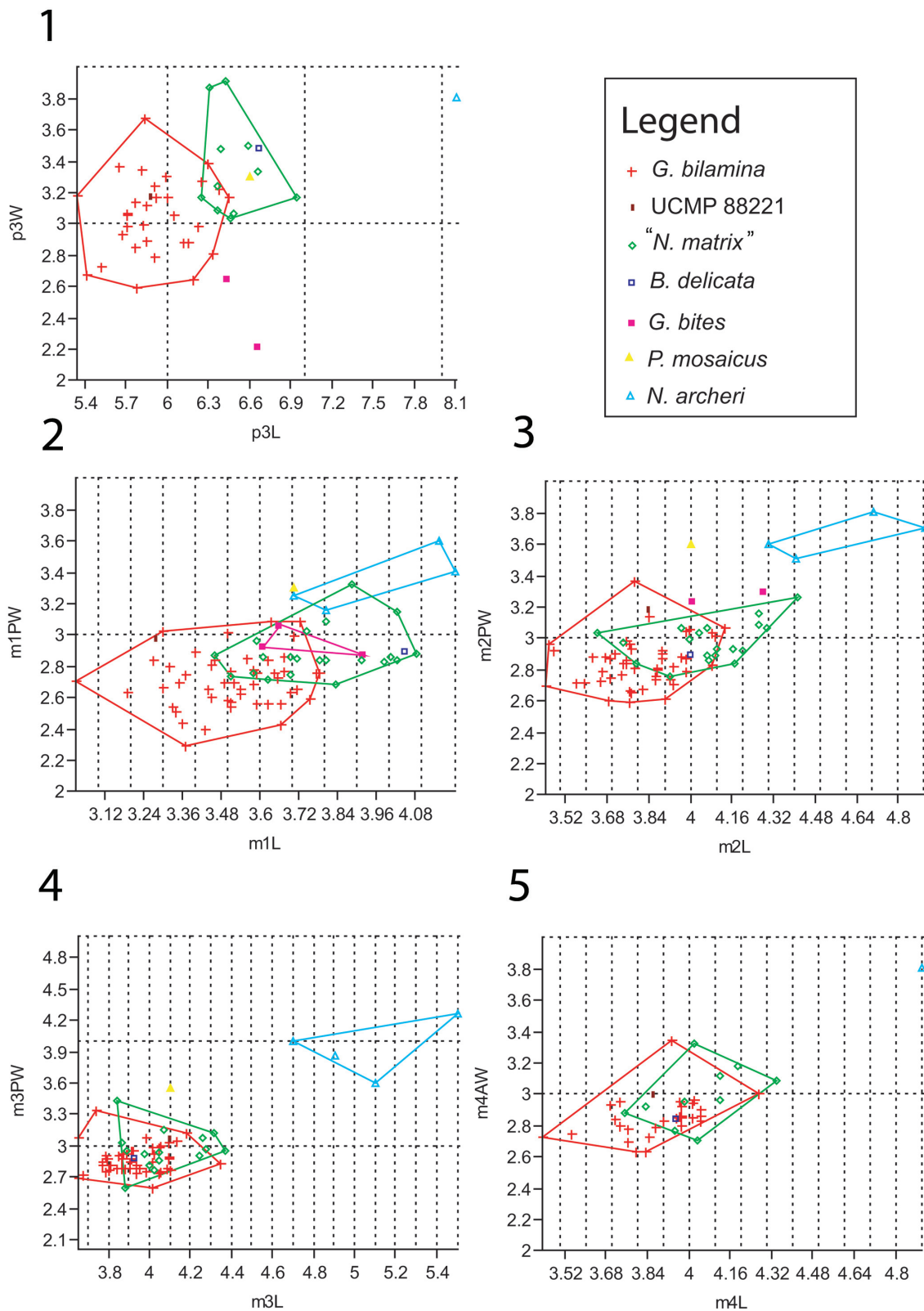
FIGURE 7. Bivariate plots of lower dentition of *Ganguroo bilamina* (+UCMP 88221 from Kutjamarpu LF)*, Ganguroo bites* n. sp., *Bulungamaya delicata, 'Nowidgee matrix', Purtia mosaicus* and *Ngamaroo archeri.* L – anteroposterior length, AW = anterior width, PW = posterior width, W = maximum width, p = premolar, m = molar.

FIGURE 8. Principle Component Analysis with convex hulls of log transformed upper (**1**) and lower (**2**) dentition measurements of *Ganguroo bilamina* (+UCMP 88221 from Kutjamarpu LF)*, Ganguroo bites* n. sp., *Bulungamaya delicata, 'Nowidgee matrix', Purtia mosaicus* and *Ngamaroo archeri.*
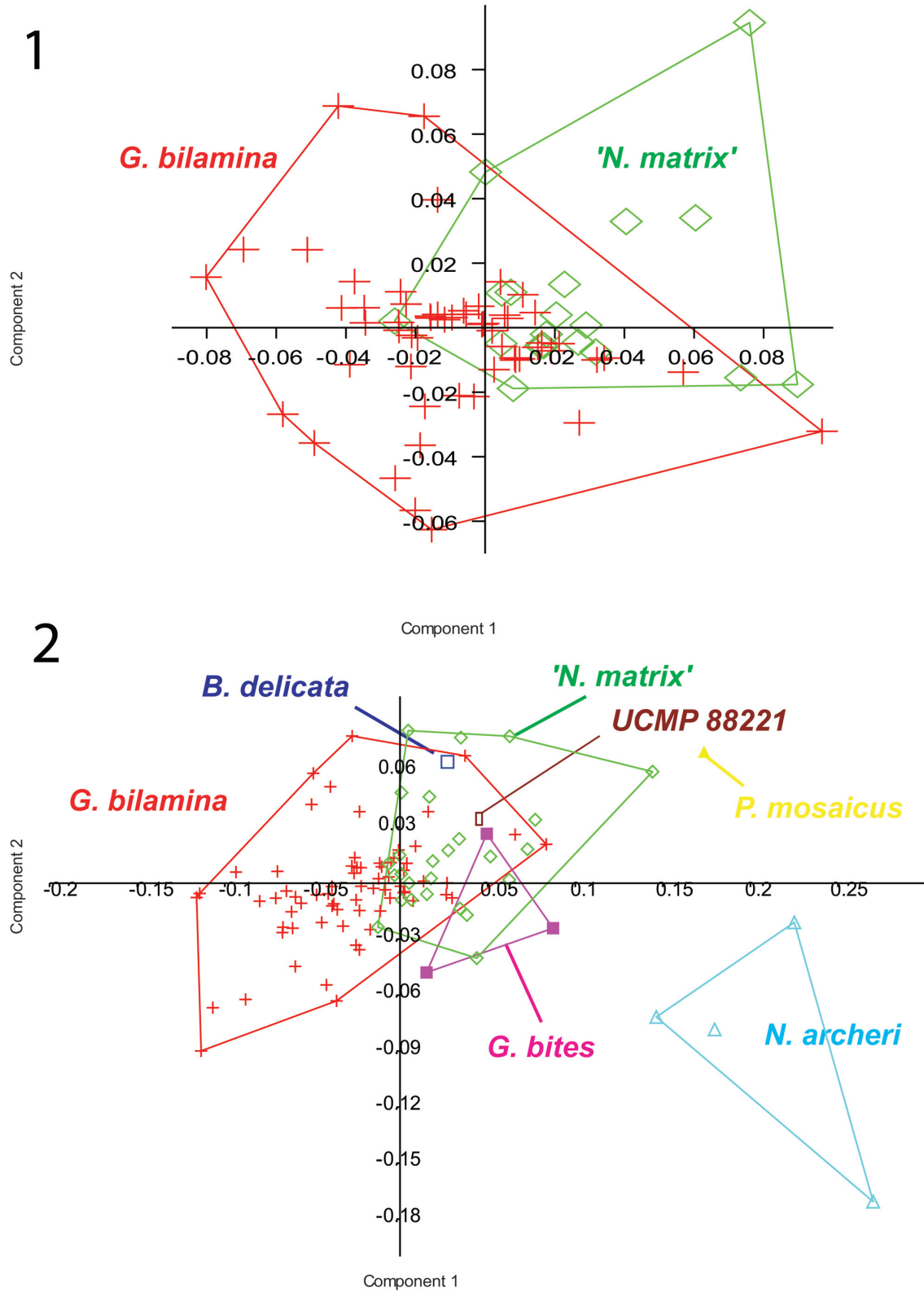
TABLE 1. Results of the Multivariate Analysis Of Variance (MANOVA) analysis showing the P-values for the mean comparison of upper (**1**) and lower (**2**) log transformed dental measurements of *Ganguroo bilamina* (+UCMP 88221 from Kutjamarpu LF)*, G. bites* n. sp., *'Nowidgee matrix'* (+*Bulungamaya delicata*) and *Ngamaroo archeri.*

1

	G. bilamina	*'N. matrix'*
G. bilamina	0	1.48E-03
'N. matrix'	1.48E-03	0

2

	G. bilamina	*G. bites*	*N. archeri*	*'N. matrix'*
G. bilamina	0	5.71E-05	9.10E-26	2.58E-07
G. bites	5.71E-05	0	Fail	0.053
N. archeri	9.10E-26	Fail	0	2.66E-08
'N. matrix'	2.58E-07	0.053	2.66E-08	0

= 11.17%, Component 4 = 8.65%, etc.). P3 length and width were the most useful measurements followed by M1 anterior and posterior width. The PCA of the lower dental variables (Figure 8) also shows significant overlap between *G. bilamina* and *N. matrix.* A specimen of *G. bilamina (*UCMP 8822) from the Leaf Locality falls within the range of Riversleigh specimens. The holotype of *Bulungamaya delicata* falls within the range of *N. matrix*. Two out of three specimens of *G. bites* fall within the range *G. bilamina* and *N. matrix,* but the third is well outside their range. *Purtia mosaicus* and *Ngamaroo archeri* are well separated. Component 1 accounts for 45.23% of the variance while Component 2 accounts for 14.62% of the variance (Component 3 =8.91%, Component 4 = 7.07%, etc.). The p3 length and width were the most useful measurements followed by m2 and m3 lengths and posterior widths.

Multivariate Analysis Of Variance (MANOVA)

When the means of log transformed dental measurements were compared using MANOVA, we found significance between comparing means of each sex of each taxon (Appendix 18.1-2) and between means of each taxon (Appendix 18.3-4). When sexes are separated, the MANOVA found no significant differences between the means of each sex of each taxon, for both upper (Appendix 18.1) and lower dentition (Appendix 18.2), with P-values ranging from 0.34 to 0.87. The MANOVA was unable to calculate p-value for the comparison between males and females of *Thylogale thetis,* as a result of a smaller sample size. In contrast, when sexes were combined as a single taxon, the MANOVA found significant differences between

taxa for both upper (Appendix 18.3) and lower dentition (Appendix 18.4), with P-values below 0.05. This suggests that when used on fossil specimens, the MANOVA should be able to differentiate between fossil taxa, but will not be able to differentiate between sexes of the same taxon.

The results of the MANOVA for the fossil specimens are shown in Table 1. The results of the MANOVA found significant differences (P-value = 1.48E-03) between *Ganguroo bilamina* and *'Nowidgee matrix'* for the mean upper dentition measurements (Table 1.1). For the mean lower dentition measurements, the results indicate that there are significant differences between all species examined (*G. bilamina* + UCMP 88221 from Kutjamarpu LF)*, G. bites*, *'N. matrix'* (+*B. delicata*) and *N. archeri*, except between *G. bites* and *N. archeri,* for which the MANOVA couldn't calculate a P-value, due to sample size (only 3 specimens for *G. bites,* and 4 for *N. archeri)*, and between *G. bites* and *'N. matrix'* were the P-value was above 0.05 (P-value=0.053).

Canonical Variates Analysis (CVA)

The results of the CVAs for the log transformed dental measurements of *Thylogale* taxa are shown in Appendix 19. Whether sexes were separated or not, the CVAs separated each group quite distinctively, with only a slight overlap between males and females *T. stigmatica* in the upper dentition. The CVA reclassifications are shown in Appendix 20. When sexes were separated, only four specimens incorrectly misclassified as the incorrect sex, but never as a different species (Appendix 20.1). When sexes were combined, not misclassification occurred (Appendix 20.2).
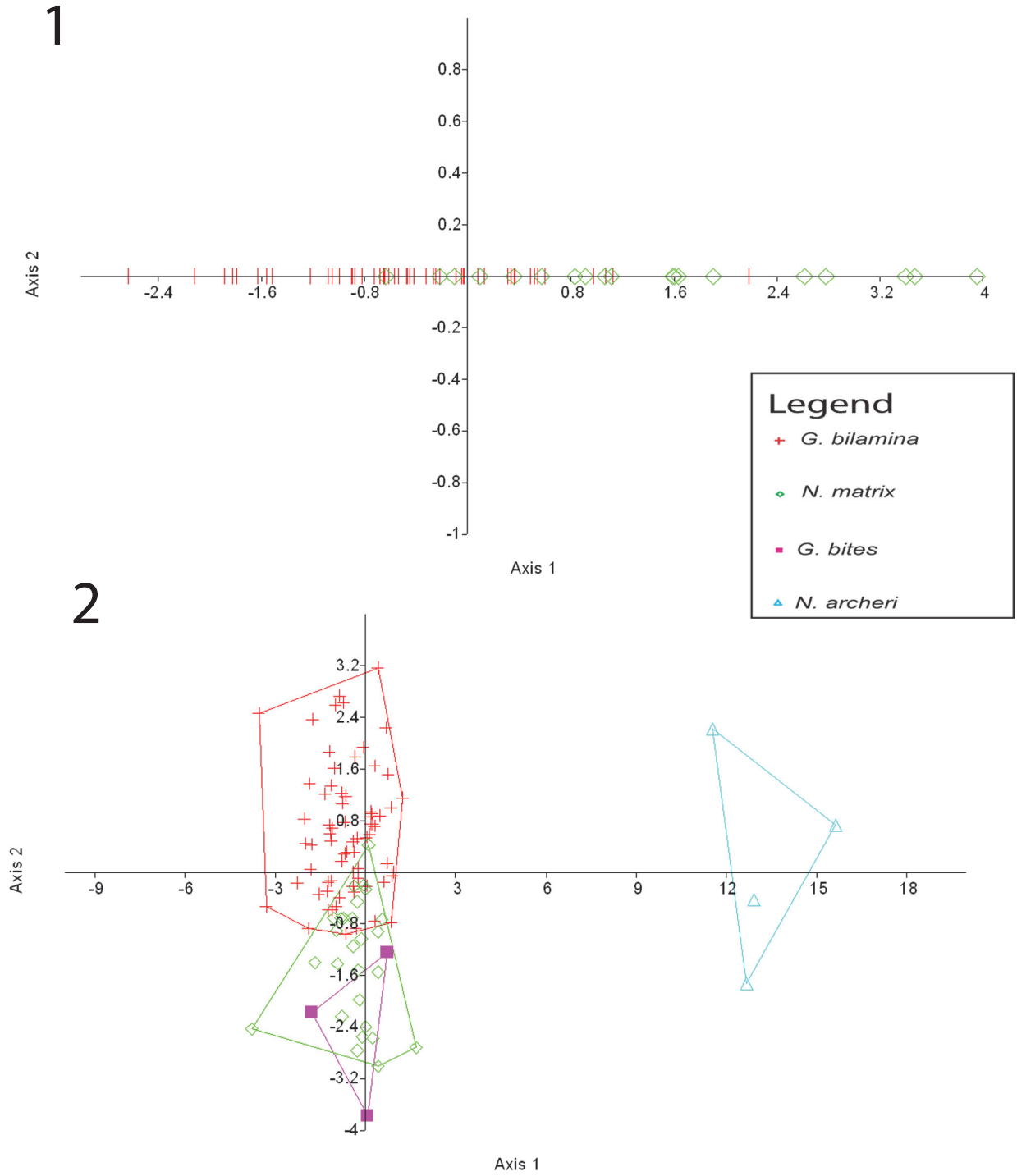
FIGURE 9. Canonical Variates Analysis with convex hulls of upper (**1**) and lower (**2**) log transformed dental measurements of *Ganguroo bilamina* (+UCMP 88221 from Kutjamarpu LF)*, Ganguroo bites* n. sp., *'Nowidgee matrix'* (+*Bulungamaya delicata*) and *Ngamaroo archeri.*

The results of the CVAs for the log transformed dental measurements of the fossil taxa are shown in Figure 9. In the upper dentition CVA (Figure 9.1), there is a lot of overlap between *Ganguroo bilamina* and *'Nowidgee matrix'*. This is also seen in the lower dentition CVA (Figure 9.2), with *G. bites* also overlapping with *'N. matrix'. Ngamaroo archeri* is, however, very well separated. CVA reclassifications are shown in Table 2. Some of the *Ganguroo bilamina* are misclassified by the CVA as *'Nowidgee matrix'* and vice versa. No *Ngamaroo archeri* is misclassified, while one specimen of *G. bites* is misclassified as *'Nowidgee matrix'*. Specimen UCMP_88221 from Kutjamarpu LF is classified by the CVA as *G. bilamina,* and the holotype of *Bulungamaya delicata,* CPC_22187, is classified as *'Nowidgee matrix'*.

Phylogenetic Analysis

Seventy-eight most parsimonious trees (tree length = 265; consistency index excluding uninformative characters = 0.4651; retention index = 0.7320) were recovered from the analysis of the morphological matrix (see Appendix 21 for matrix). The strict consensus tree of these is given in Figure 10, with bootstrap (above branches) and Bremer (below branches) support values.

The strict consensus is highly unresolved, with few branches supported by high bootstrap or Bremer values. Macropodoidea is divided in two major clades, one comprising macropodines, sthenurines, Riversleigh fossil taxa and potoroines (bootstrap = 67%) and the other comprising balbarids and hypsiprymnodontids (bootstrap = <50%). The relationship between Riversleigh fossil taxa (*Bulungamaya delicata, Ganguroo bilamina, G. bites* and *Wabularoo naughtoni*) and potoroines (*Bettongia penicillata, B. moyesi, Potorous tridactylus, Purtia mosaicus, Ngamaroo archeri* and *Wakiewakie lawsoni*) is unresolved, with monophyly of Potoroinae not recovered while *P. mosaicus, N. archeri* and *W. lawsoni* form a clade distinct from that of other potoroines (bootstrap =<50%). *Wanburoo hilarus* is recovered as the sister taxon (bootstrap = 59%, Bremer = +2) to all macropodines and sthenurines. The macropodine and sthenurine clades are recovered with moderate support (bootstrap = 61%, Bremer = +2) and resolution within each clade. The relationship of Riversleigh fossil taxa (*Bulungamaya delicata, Ganguroo bilamina, G. bites* and *Wabularoo naughtoni*) within Macropodoidea remains uncertain.

DISCUSSION

Coefficients of variation of dental dimensions of a single, mixed-sex population, usually falls between 0 and 10 (Simpson et al., 1960).The results of our metric analyses demonstrate that even though p3 and P3 are the most variable teeth in terms of length and width (CV values >10) measures, they remain the most useful teeth to distinguish species of *Thylogale* in thebivariate plots, Principle Component Analysis (PCA) and Canonical Variates Analysis (CVA). These results are consistent with the metric analyses of species of *Macropus* in Bartholomai (1971). However, Bartholomai (1971) urges that all cheekteeth should be considered together, taking into account both the variation in size and morphological characters.

Dental measurements for *Ganguroo bilamina* are within the range expected from a single species (CV values <10) for both the lower and the newly described upper dentition (Simpson et al., 1960). Molar measurements significantly overlap with other fossil species (e.g., *Bulungamaya delicata/'Nowidgee matrix'* and *Ganguroo bites*), although anterior molars are generally smaller in size and upper and lower third premolar measurements overlap very little with *Bulungamaya delicata/'Nowidgee matrix'* and not at all with *G. bites*. Morphologically, *G. bilamina* differs from the bunolophodont *B. delicata/N. matrix* in being completely bilophodont (sensu Cooke, 1997a) and differs from *G. bites* in having seven cuspids instead of eight on p3, no paraconid present on any molars and a buccal crest from the entoconid, which is evident in juveniles but worn away in adults. Both morphology and size variation strongly support G. *bilamina* being treated as a species distinct from *B. delicata/ 'N. matrix'* and *G. bites.*

While *Bulungamaya delicata* (Flannery et al., 1983) and *'Nowidgee matrix'* (Cooke, 1997a) were described as separate species in part because the type specimens of *B. delicata* are heavily worn, making it difficult to compare their morphology with relatively unworn specimens. Here we argue that they represent the same species. First, metric analyses do not support the view that there are two species involved. All dental measurements of *B. delicata* fall within the range of *'N. matrix'* (see bivariate plots, Figures 7). In both the PCA and CVA, *B. delicata* wfell within the range of *'N. matrix'* and was reclassified by the CVA as *'N. matrix'* (Figures 8, 9, Table 2). Combined univariate statistics for the two species had coefficient of variation values within the range of a single species (CV = <10, Appendices 4, 5) and the MANOVA (Table 1) sug-

TABLE 2. Results of the Canonical Variates Analysis (CVA) reclassification using log transformed dental measurements of fossil specimens, for the upper (**1**) and lower (**2**) dentition. Group 1 = *Ganguroo bilamina*; group 2 = *'Nowidgee matrix'*; group 3 = *Ngamaroo archeri*; group 4 = *G. bites*. Incorrect reclassifications are highlighted in grey.
12

	Upper dentition			Lower dentition	
Specimen	Given group	CVA Classification	Specimen	Given group	CVA Classification
QMF56318	1	1	QMF19870	1	1
QMF56995	1	1	QMF19868	1	1
QMF19696	1	2	QMF19966	1	1
QMF19696	1	1	QMF30400	1	1
QMF19958	1	1	QMF56996	1	1
QMF20705	1	1	QMF19607	1	1
QMF19900	1	1	QMF20248	1	1
QMF19695	1	1	QMF20254	1	1
QMF20253	1	1	QMF23486	1	2
QMF19861	1	1	QMF20246	1	1
QMF19976	1	1	QMF20019	1	1
QMF19957	1	1	QMF56995	1	1
QMF19857	1	1	QMF19903	1	1
QMF19975	1	1	QMF56254	1	1
QMF19959	1	1	QMF56259	1	2
QMF20017	1	1	QMF24744	1	1
QMF56990	1	1	QMF20006	1	1
QMF30436	1	1	QMF36351	1	1
QMF30343	1	1	QMF19988	1	1
QMF36230	1	1	QMF19844	1	1
QMF19668	1	1	QMF24190	1	2
QMF19692	1	1	QMF20039	1	1
QMF234604	1	1	QMF30396	1	1
QMF19987	1	1	QMF19642	1	1
QMF23202	1	1	QMF30397	1	1
QMF20269	1	2	QMF20293	1	1
QMF56993	1	1	QMF56999	1	1
QMF19801	1	1	QMF20271	1	1
QMF19673	1	1	QMF19643	1	2
QMF56992	1	1	QMF20295	1	1
QMF19985	1	2	QMF19947	1	1
QMF19885	1	1	QMF56991	1	1
QMF19687	1	1	QMF20272	1	1
QMF19651	1	1	QMF19640	1	1

TABLE 2 (continued).

QMF19689	1	1	QMF19646	1	1
QMF19629	1	1	QMF19688	1	1
QMF19674	1	1	QMF19814	1	1
QMF52814	1	2	QMF30399	1	1
QMF52814	1	1	QMF19591	1	1
QMF57020	1	1	QMF19810	1	1
QMF57020	1	1	QMF19835	1	1
QMF20261	1	1	QMF57022	1	1
QMF19589	1	1	QMF19836	1	1
QMF19617	1	1	QMF57021	1	1
QMF19590	1	1	QMF56998	1	1
QMF24219	1	2	QMF19834	1	1
QMF20163	1	1	QMF19827	1	2
QMF56256	1	2	QMF20082	1	1
QMF56258	1	1	QMF19597	1	2
QMF56265	1	1	QMF24480	1	1
QMF56265	1	1	QMF56997	1	1
QMF24475	1	2	QMF20108	1	1
QMF24476	1	1	QMF20109	1	1
QMF50518	1	1	QMF19915	1	1
QMF56261	1	1	QMF19602	1	1
QMF56255	1	2	QMF50519	1	1
QMF56255	1	1	QMF50519	1	1
QMF24216	1	1	QMF24050	1	1
QMF56263	1	1	QMF30721	1	1
QMF57023	2	2	QMF20081	1	1
QMF19965	2	1	QMF36364	1	1
QMF19954	2	2	QMF24477	1	1
QMF19953	2	2	QMF30398	1	1
QMF23491	2	2	QMF56257	1	1
QMF20285	2	2	QMF24482	1	2
QMF19675	2	2	QMF31405	1	1
QMF20310	2	1	QMF56260	1	1
QMF29702	2	1	QMF36363	1	2
QMF57024	2	2	QMF36470	1	1
QMF20011	2	2	QMF56264	1	1
QMF19986	2	1	UCMP_88221	1	1
QMF19619	2	2	CPC_22187	2	2
QMF19616	2	2	QMF30390	2	2
QMF19939	2	2	QMF22761	2	2
QMF56989	2	2	QMF19961	2	2

TABLE 2 (continued).

QMF19918	2	2		QMF20255	2	2
QMF30831	2	1		QMF30392	2	2
QMF24478	2	2		QMF30394	2	2
				QMF19962	2	1
				QMF19984	2	2
				QMF19974	2	1
				QMF30723	2	2
				QMF24651	2	2
				QMF30718	2	2
				QMF57012	2	2
				QMF30393	2	2
				QMF20080	2	2
				QMF20069	2	2
				QMF19937	2	2
				QMF30391	2	2
				QMF56988	2	2
				QMF19579	2	2
				QMF24184	2	2
				QMF19586	2	2
				QMF24191	2	2
				QMF20165	2	1
				QMF56253	2	2
				QMF19991	2	2
				SAMP23626	3	3
				SAMP27817	3	3
				SAMP27818	3	3
				SAMP31834	3	3
				QMF23776	4	4
				QMF23775	4	2
				QMF23777	4	4

gested that the mean of combine specimens *B. delicata* and '*N. matrix*' were significantly different from other taxa. Morphologically, while it is very difficult to compare the worn type specimens of *B. delicata* to other specimens, several features are shared between *B. delicata* and '*N. matrix*', suggesting synonymy of these species (Figures 3, 4). These features are: the occlusal surface of i1 reaches the level of occlusal plane of the molars (Figure 3; it is below the molar occlusal plane in *G. bilamina*); p3 transcristids are relatively coarse (Figures 3, 4; transcristids are much finer in spe-

cies of *Ganguroo*); cristid obliqua connects to protoconid (visible on m3 of the holotype of *B. delicata*); buccal crest from the entoconid does not connect to the hypoconid (also visible on m3 in the holotype of *B. delicata*); and the talonid of m4 is significantly smaller than the trigonid (contra the condition in species of *Ganguroo*). The lower molar proportions of type specimens of *B. delicata* from Riversleigh's D and G Sites are almost identical to the only known specimen of '*N. matrix*' from White Hunter Site. All three of these sites are interpreted to be late Oligocene in age (Archer et al., 1989,
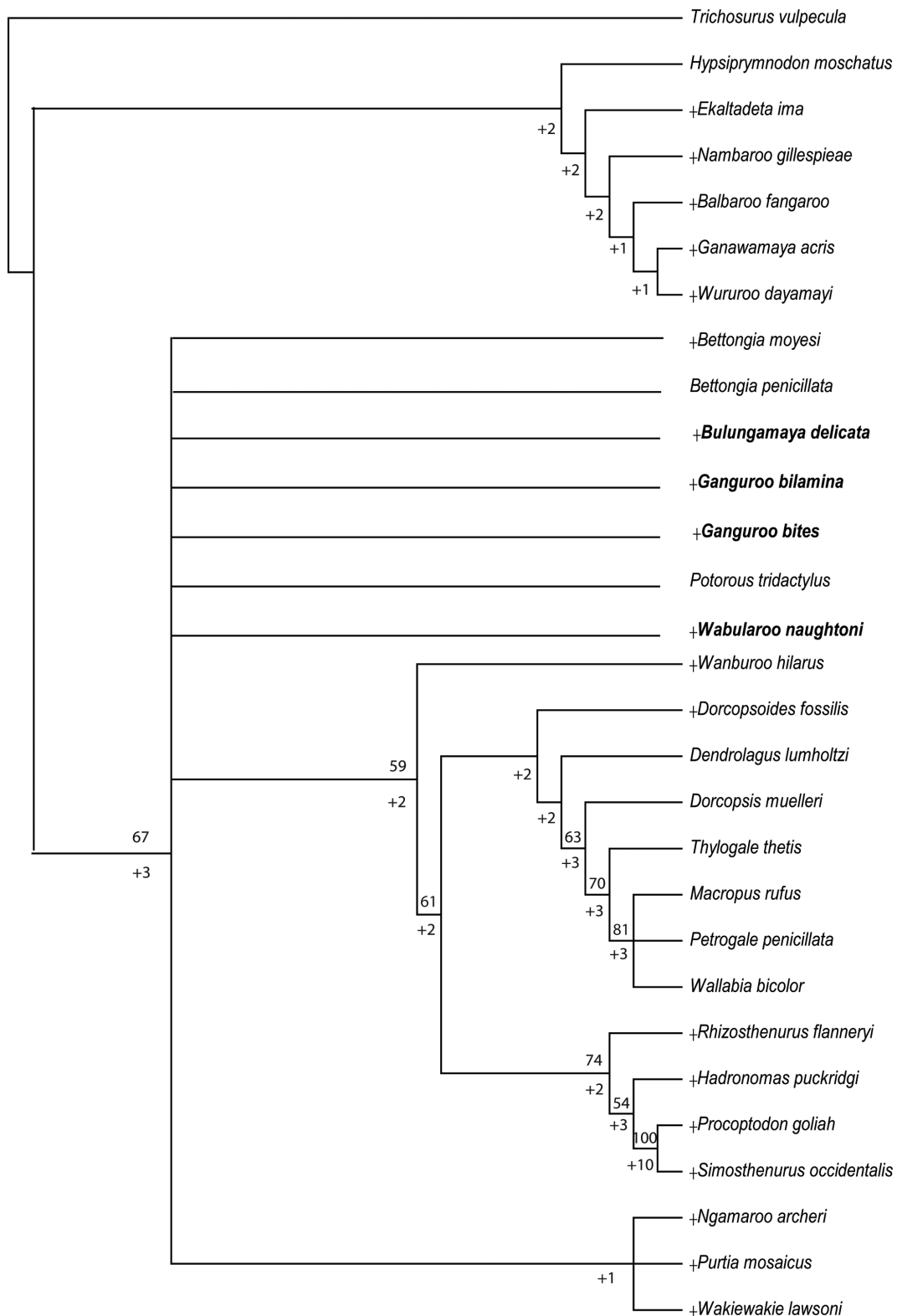
FIGURE 10. Phylogenetic relationships of *Bulungamaya delicata, Ganguroo bilamina, Ganguroo bites* and *Wabularoo naughtoni* (highlighted in bold), based on 108 character craniodental matrix. Fossil taxa are indicated by †. Strict consensus of 78 most parsimonious trees (tree length = 265; consistency index excluding uninformative characters = 0.4651; retention index = 0.732) from maximum parsimony analysis of the matrix. Numbers above branches represent bootstrap values (1000 replicates); numbers below branches represent decay indices.

1997; Arena, 2004; Travouillon et al., 2006, 2011). Considering the overall similarity in size and morphology, we propose that '*Nowidgee matrix*' be regarded as a junior synonym of *Bulungamaya delicata.*

The phylogenetic analysis failed to resolve the relationship of basal macropodids to other macropodoids. *Ganguroo bilamina, G. bites, Bulungamaya delicata* and *Wabularoo naughtoni* were recovered as a clade containing potoroines and macropodines+sthenurines, but the relationship was not resolved. Kear et al. (2007) and Kear and Pledge (2008) recovered 'bulungamayines' as a paraphyletic group, more closely related to macropodines than potoroines, but with no support (bootstrap values = <50%). They recommended 'Bulungamayinae' to be treated as *incertae sedis.* However, there are some issues with the character coding for 'bulungamayines' in those studies. First, characters scored for *Wabularoo naughtoni* include cranial and upper dentition scores based on undescribed material. Second, characters scored for *G. bilamina* include postcranial scores belonging to another species from AL90 Site, *Ganguroo* sp. 2, which is also undescribed. Third, characters scored for *B. delicata* include cranial and upper dentition scores also based on undescribed specimens but which in this case have been determined here to represent *G. bilamina.*

In contrast, Prideaux and Warburton (2010), who only included in their analysis *Ganguroo bilamina* and '*Nowidgee matrix*', recovered '*N. matrix*' as the sister group to all macropodids (lagostrophines, sthenurines and macropodines), and *G. bilamina* as the sister group to sthenurines and macropodines with stronger support values (bootstrap = >50%). It is noteworthy that Prideaux and Warburton (2010) completely rescored *G. bilamina* and '*N. matrix*' based on type material assigned to both species by Cooke (1997a), but they did include postcranials assigned incorrectly to *G. bilamina* by Kear et al. (2001a).

New material of *Ganguroo bilamina* described in this paper may also shed some light on its relationship to other macropodoids. The flat frontal region observed in *G. bilamina* is also present in skulls of *Ganguroo* sp. 2. This feature may be a synapomorphy for species of *Ganguroo* although this region of the skull is not preserved in specimens of *G. bites.* Some features of the skull of *G. bilamina*, however, are almost certainly plesiomorphic for macropodoids. For example, absence of flexion of the skull in the basicranial and rostral regions, smooth transition of the zygoma to the cheek region and lack of development of the masseteric process are also features of hypsiprymnodontids, potoroines and balbarids (Kear and Cooke, 2001). However, *G. bilamina* shares derived features with macropodines including a broad parietal-alisphenoid contact and an alisphenoid contribution to the ventral floor of the secondary foramen ovale which suggest a closer relationship with macropodines (Kear and Cooke, 2001).

Upper molars of *G. bilamina* are also more derived than *Bulungamaya delicata* in protoloph morphology, being bilophodont rather than bunolophodont. The M1 of *G. bilamina* has a 'forelink' derived from the preprotocrista, which contributes a lingual component to the protoloph crest before turning anteriorly. In contrast, in *B. delicata* the preprotocrista makes no contribution to the protoloph crest. The M1 of *G. bilamina*, however, retains a remnant of stylar cusp D in the form of a stylar crest which is absent in *B. delicata*.

The neometaconule of *Ganguroo bilamina* occurs also in *Bulungamaya delicata*. It is also common in relatively derived balbarines (Cooke, 2000) and relatively derived macropodids such as sthenurines (Prideaux, 2004). Tedford and Woodburne (1987) note that the neometaconule is a neomorphic structure in quadritubercular upper molars of diprotodontian marsupials. In agreement, it is therefore more parsimonious to presume that the neometaconule of macropodoids is a plesiomorphic feature rather than independently developed in the different macropodoid lineages in which it occurs. Absence of this feature in some balbarines and basal macropodids would accordingly be the result of secondary loss rather than a plesiomorphic macropodoid condition.

Lower molars of *Ganguroo bilamina* are clearly more derived than those of species of *Bulungamaya delicata* in terms of hypolophid formation. In *G. bilamina*, the entoconid is linked to the hypoconid by the posthypocristid, which has become transversely orientated and elevated, in addition to a second crest that departs bucally from the entoconid and is sometimes present in juveniles (contra Cooke, 1997a). This situation contrasts with the condition in balbarines where both a buccal crest from the entoconid and the lingually displaced posthypocristid contribute to the hypolophid (Cooke, 1997c). While both balbarines and macropodids have achieved bilophodonty in lower molars, the process of doing so appears to be the result of parallel evolution. In contrast, loph formation in upper molars has apparently proceeded in

similar ways in both groups. The preprotocrista contributes the lingual component of the protoloph and continues anteriorly to form the forelink (Cooke, 2000).

Cooke (1997b) provided the first species occurrence list of Riversleigh macropodoids, which was later updated in Archer et al. (2006) and Travouillon et al. (2011). In the course of compiling data for the present paper, we reviewed all available macropodoid specimens from Riversleigh (Table 3) other than hypsiprymnodontids and balbarids, which will be the subject of a separate review. A number of taxa listed in Cooke (1997b), Archer et al. (2006) and Travouillon et al. (2011) have been left unchanged, removed from or modified in our species lists here for the following reasons.

Gumardee pascuali is probably a large potoroine, as described by Flannery et al. (1983) on the basis of a single worn maxilla from D Site which contained an elongated P3, typical of potoroines. No further material has been reported until now. Cooke (1997b) reported the presence of an undescribed species, '*Nowidgee'* sp. 2, based on two dentaries from the White Hunter Site. New material from White Hunter Site, including an almost complete skull and several maxillae and dentaries, perfectly matches *G. pascuali*. The two dentaries referred by Cooke (1997b) to '*Nowidgee'* sp. 2 also appear to be referrable to *G. pascuali*. Added support for this conclusion comes from the fact that the dentaries perfectly occlude with the maxillae, corresponding precisely in size and morphology (bunolophodont dentition). Hence we conclude that '*Nowidgee'* sp. 2 is synonymous with *G. pascuali* (Table 3) and should no longer used in the literature, at least until it is formally described.

Wabularoo naughtoni was first described by Archer (1979) on the basis of a dentary from D Site and a p3 from G Site. Flannery et al. (1984) reported an additional specimen from D Site. Cooke (1997b) reported the occurrence of this species from undescribed specimens in White Hunter Site as well as six younger Faunal Zone B sites. After re-examining this material, we do not agree with Cooke (1997b) that these specimens belong to *W. naughtoni,* as none possesses the distinctive enlarged p3 characterising this species, apart from the specimen from White Hunter Site. These species occurrences should not be used at least until the material is formally described.

Wakiewakie lawsoni was described by Woodburne (1984) on the basis of a dentary and two P3s from the Kutjamarpu Local Fauna from Lake Nga-

pakaldi in northern South Australia. This species was also reported from Riversleigh on the basis of a single Faunal Zone B dentary from Upper Site (Godthelp et al., 1989).

Bulungamaya delicata, first described by Flannery et al. (1983) on the basis of specimens from D Site and G Site, was also reported by Cooke (1997b) from a number of Faunal Zone A, B and C specimens. After reviewing these specimens in the context of the present review, we determined that some of these additional specimens appear to represent other taxa (e.g., *Ganguroo bilamina* and *G.* sp. 2). While it is clear that *B. delicata* is represented by specimens from Faunal Zones A and B, the only Faunal Zone C deposit occurs in the Keith's Chocky Block Site (KCB), which is a vertical fissure fill. As noted by several authors (e.g., Creaser, 1997; Archer et al., 1997; Travouillon et al., 2006, 2011), the KCB Site may have been collecting fossils for a longer period of time than other sites and potentially taxa from both Faunal Zones B and C.

Cooke (1997a) described *Ganguroo bilamina* based on dentaries from Faunal Zone B sites. Here, we describe additional material from this species and reassign specimens from the Bitesantennary Site originally assigned to *G. bilamina* to a new species, *G. bites.* As noted above, all specimens of *G. bilamina* occur in Faunal Zone B, except for Cadbury's Kingdom (CK) Site, which was previously thought to be a Faunal Zone C site (Travouillon et al., 2006, 2011). However, assignment of the CK faunal assemblage to Faunal Zone C had low support (<50%, Travouillon et al., 2011). Eight of the nine species present in this site are present in at least Zones B and C (and in some cases all Faunal Zones). *Nimiokoala greystanesi* is only present in Faunal Zone B and Cadbury's Kingdom, as is *Priscakoala lucyturnbullae* (Black et al., 2012). Additionally, while reviewing the whole collection, *Balbaroo fangaroo* was identified from Cadbury's Kingdom, which otherwise only occurs in Faunal Zone B, while a more derived species occurs in Faunal Zone C (*Balbaroo* sp. 4 of Cooke, 1997b). Similarly, the relatively derived species of *Ganguroo, Ganguroo* sp. 2, occurs in Faunal Zones C and D, but not B. There is, on balance, more support for referring the CK assemblage to Faunal Zone B than C, suggesting that *G. bilamina* is restricted to Faunal Zone B (Table 3). The presence of *G. bilamina* in the Kutjamarpu Local Fauna strengthens biocorrelations with Riversleigh's Faunal Zone B. A description of *Ganguroo* sp. 2 is in progress.

TABLE 3. Site occurrence (serriated) of pre-Pliocene Riversleigh basal macropodid species, excluding hypsiprymno-dontids and balbarids.

Species	Faunal Zone A			FZA?	Faunal Zone B												FZB/C?	Faunal Zone C																		FZD	TOTAL
	G Site	D Site	White Hunter Site	Judy's Jumping Joint Site	Dirk's Tower Site	BitesAntennary Site	Cadbury's Kingdom Site	Camel Sputum Site	Inabeyance Site	Judith Horizontalis Site	Mike's Menagerie Site	Mike's Potato Patch Site	Neville's Garden Site	RSO Site	Upper Site	Wayne's Wok Site	KCB Site	AL90 Site	Cleft Of Ages Site	Dome Site	Gag Site	Henk's Hollow Site	Two Trees Site	Jim's Carousel Site	Jim's Jaw Site	Last Minute Site	Main Site	NJC08 Site	Rick Sausage Site	Melody's Maze Site	Arachnid Ridge	Angela's Sinkhole Site	Golden Steph Site	Jaw Junction Site	Skull Site	Encore Site	
Rhizosthenurus flanneryi																																				1	1
Wanburoo hilarus																	1	1	1	1	1	1	1	1	1	1	1	1	1								13
Bettongia moyesi																						1	1														2
Ganguroo sp. 2																	1	1	1	1	1	1			1	1	1	1	1	1	1	1	1	1	1	1	18
G. bilamina							1	1	1	1	1	1	1	1	1	1																					10
G. bites						1																															1
Bulungamaya delicata	1	1	1	1	1			1					1	1	1	1																					10
Wakiewakie lawsoni															1																						1
Wabularoo naughtoni	1	1	1																																		3
Gumardee pascuali		1	1																																		2
Total	2	3	3	1	1	1	1	2	1	1	1	1	2	1	3	2	3	2	2	2	2	3	1	2	1	2	2	2	2	1	1	1	1	1	1	2	

The suggestion that *Ganguroo bilamina* and *Bulungamaya delicata* are present in the Price Is Right LF (Archer et al., 2006) is not supported here because specimens used to identify these two species are larger and morphologically distinct. All specimens from the Price Is Right Site examined during the present study appear to represent *Balbaroo fangaroo*, *Ganawamaya acris* and a new species related to *Gumardee pascuali.*

Bettongia moyesi was described on the basis of an associated skull and dentary from the Two Trees Site on the Gag Plateau at Riversleigh as the earliest record of a modern potoroine genus (Flannery and Archer, 1987b). Since then, another dentary has been recovered from the Henk's Hollow Site, confirming its presence in Faunal Zone C (Archer et al., 2006). Two specimens from the Melody's Maze Site, also on the Gag Plateau, may represent a new potoroine (Table 3).

Wanburoo hilarus was described as a 'bulungamayine' on the basis of several dentaries and upper teeth from Faunal Zone C sites and Encore Site (Cooke, 1999; gen. *Wan.* sp. 1 in Cooke, 1997b). However, Prideaux and Warburton (2004) suggest that it may be in fact a sthenurine. In our review of Riversleigh material, we have identified new specimens referable to this species, including a near complete skull. Dental specimens from the Encore Site (gen. *Wan.* sp. 2 in Cooke 1997b), however, are synonymous with *Rhizosthenurus*

flanneryi (Kirkham, personal commun., 2013), which was first described as *Wanburoo* sp., then renamed in a following publication, based on post-cranial material from the same site (Kear et al., 2001b; Kear, 2002). Cooke (1997b) also notes an undescribed species, *Wanburoo* sp. 2, from the Encore, Last Minute and Henk's Hollow Sites. However, specimens of *Wanburoo* sp. 2 from the Encore Site are synonymous with *R. flanneryi* and from the Last Minute and Henk's Hollow Sites with *W. hilarus.* A complete description of the skull and dentition of *R. flanneryi* is currently in progress (Kirkham et al., in prep.).

CONCLUSION

Based on morphological assessment and metric analyses, '*Nowidgee matrix*' is synonymised with *Bulungamaya delicata.* This bunolophodont species is now known from upper and lower dentitions, from several of Riversleigh's Faunal Zone A and B sites as well as Keith's Chocky Block Site (arguably Faunal Zone C but as a vertical fissure fill it may have also accumulated fossils from Faunal Zone B). We have described additional material for *Ganguroo bilamina,* including the previously unknown skull and upper dentition, and described a new species, *G. bites*, from the Bitesantennary Site. These two species are currently restricted to Faunal Zone B. Our phylogenetic analysis was unable to resolve the interrelationships of basal macropodids. However, cranial and dental morphology of *G. bilamina* suggest closer affinities with macropodines than potoroines. Finally, we have revised understanding about some of the other macropodoid taxa in pre-Pliocene Riversleigh sites.

ACKNOWLEDGMENTS

REFERENCES

Aplin, K.P. and Archer, M. 1987. Recent advances in marsupial systematics with a new syncretic classification, p. xv-lxxii. In Archer, M. (ed.), *Possums and Opossums, Studies in Evolution*. Surrey Beatty and Sons, Sydney, Australia.

Archer, M. 1979. *Wabularoo naughtoni* gen. et sp. nov., an enigmatic kangaroo (Marsupialia) from the middle Tertiary Carl Creek Limestone of northwestern Queensland. Results of the Ray E. Lemley Expeditions, part 4. *Memoirs of the Queensland Museum,* 19:299-307.

Archer, M. 1984. The Australian mammal radiation, p. 585-625. In Archer, M. and Clayton, G. (eds.), *Vertebrate Zoogeography and Evolution in Australasia*. Hesperian Press, Western Australia, Carlisle.

Archer, M., Godthelp, H., Hand, S.J., and Megirian, D. 1989. Fossil mammals of Riversleigh, northwestern Queensland: preliminary overview of biostratigraphy, correlation and environmental change. *Australian Zoolologist*, 25:29-65.

Archer, M., Hand, S.J., Godthelp, H., and Creaser, P. 1997. Correlation of the Cainozoic sediments of the Riversleigh World Heritage fossil property, Queensland, Australia, p. 131-152. In Aguilar, J.-P., Legendre, S., and Michaux, J. (eds.), *Actes du Congrès BiochroM'97*. École Pratique des Hautes Études, Institut de Montpellier, France.

Archer, M., Arena, D.A., Bassarova, M., Beck, R.M.D., Black, K., Boles, W.E., Brewer, P., Cooke, B.N., Creaser, P., Crosby, K., Gillespie, A., Godthelp, H., Hand, S.J., Kear, B.P., Louys, J., Morrell, A., Muirhead, J., Roberts, K.K., Scanlon, J.D., Travouillon, K.J., and Wroe, S. 2006. Current status of species- level representation of faunas from selected fossil localities in the Riversleigh World Heritage Area, northwestern Queensland. *Alcheringa Special Issue*, 1:1-17.

Arena, D.A. 2004. *The geological history and development of the terrain at the Riversleigh World Heritage Area during the middle Tertiary*. Unpublished PhD Thesis, University of New South Wales, Sydney, Australia.

Bartholomai, A. 1971. Morphology and variation of the cheek teeth in *Macropus giganteus* Shaw and *Macropus agilis* (Gould). *Memoirs of the Queensland Museum,* 16:1-18.

Beck, R.M.D., Godthelp, H., Weisbecker, V., Archer, M., and Hand, S.J. 2008. Australia's oldest marsupial fossils and their biogeographical implications. *PloS ONE,* 3(3):e1858. doi:10.1371/journal.pone.0001858

Black, K.H., Archer, M., and Hand, S.J. 2012. New Tertiary koala (Marsupialia,

Phascolarctidae) from Riversleigh, Australia, with a revision of phascolarctid phylogenetics, paleoecology, and paleobiodiversity. *Journal of Vertebrate Paleontology,* 32:125-138.

Case, J.A. 1984. A new genus of Potoroinae (Marsupialia: Macropodidae) from the Miocene Ngapakaldi Local Fauna, South Australia, and a definition of the Potoroinae. *Journal of Paleontology*, 58:1074-1086.

Cooke, B.N. 1997a. New Miocene bulungamayine kangaroos (Marsupialia: Potoroidae) from the Riversleigh, northwestern Queensland. *Memoirs of the Queensland Museum,* 41:281-294.

Cooke, B.N. 1997b. Biostratigraphic implications of fossil kangaroos at Riversleigh, northwestern Queensland. *Memoirs of the Queensland Museum*, 41:295-302.

Cooke, B.N. 1997c. Two new balbarine kangaroos and lower molar evolution within the subfamily. *Memoirs of the Queensland Museum*, 41:269-280.

Cooke, B.N. 1999. *Wanburoo hilarus* gen. et sp. nov., a lophodont bulungamayine kangaroo (Marsupialia: Macropodoidea: Bulungamayinae) from the Miocene deposits of Riversleigh, northwestern Queensland. *Records of the Western Australian Museum, Supplement* 57:239-253.

Cooke, B.N. 2000. Cranial remains of a new species of balbarine kangaroo (Marsupialia: Macropodoidea) from the Oligo-Miocene freshwater limestone deposits of Riversleigh World Heritage Area, northern Australia. *Journal of Paleontology*, 74:317-326.

Cooke, B.N., Travouillon, K.J., Archer, M., and Hand, S.J. in review. *Ganguroo robustiter* sp. nov. (Macropodoidea, Marsupialia), a middle to early late Miocene macropodid from Riversleigh World Heritage Area, Australia. *Acta Palaeontologica Polonica.*

Creaser, P. 1997. Oligocene–Miocene Sediments of Riversleigh: the potential significance of topography. *Memoirs of the Queensland Museum*, 41:303-314.

Flannery, T.F. and Archer, M. 1987a. *Hypsiprymnodon bartholomaii* (Potoroidae: Marsupialia), a new species from the Miocene Dwornamor Local Fauna and a reassessment of the phylogenetic position of *H. moschatus*, p. 749-758. In Archer, M. (ed.), *Possums and Opossums: Studies in Evolution*. Surrey Beatty and Sons, Sydney.

Flannery, T.F. and Archer, M. 1987b. *Bettongia moyesi*, a new and plesiomorphic kangaroo (Marsupialia: Potoroidae) from Miocene sediments of northwestern Queensland, p. 759-767. In Archer, M. (ed.), *Possums and Opossums: Studies in Evolution*. Surrey Beatty and Sons, Sydney.

Flannery, T.F., Archer, M., and Plane, M. 1983. Middle Miocene kangaroos (Macropodoidea: Marsupialia) from three localities in northern Australia with a description of two new subfamilies. *Bureau of Mineral Resources Journal of Australian Geology and Geophysics*, 7:287-302.

Flannery, T.F., Archer, M., and Plane, M. 1984. Phylogenetic relationships and a reconsideration of higher level systematics within the Potoroidae (Marsupialia). *Journal of Paleontology*, 58:1087-1097.

Flower, W.H. 1869. Remarks on the homologies and notations of the teeth of the Mammalia. *Journal of Anatomy and Physiology*, 3:262-278.

Godthelp, H., Archer, M., Hand, S.J., and Plane, M.D. 1989. New potoroine from Tertiary Kangaroo Well Local Fauna, N.T. and description of upper dentition of potoroine *Wakiewakie lawsoni* from Upper Site Local Fauna, Riversleigh. *Conference on Australasian Vertebrate Evolution, Palaeontology and Systematics (CAVEPS) Abstracts*:6.

Hammer, Ø., Harper, D.A.T., and Ryan, P.D. 2001. PAST: Palaeontological statistics software package for education and data analysis. *Palaeontologia Electronica,* 4.1.4:9pp., 178KB; http://palaeo-electronica.org/2001_1/past/issue1_01.htm

Kear, B.P. 2002. Phylogenetic implications of macropodid (Marsupialia: Macropodoidea) postcranial remains from Miocene deposits of Riversleigh, Northwestern Queensland. *Alcheringa*, 26:299-318.

Kear, B.P. and Cooke, B.N. 2001. A review of macropodoid systematics with the inclusion of a new family. *Memoirs of the Association of Australasian Palaeontologists*, 25:83-101.

Kear, B.P. and Pledge, N. S. 2008. A new fossil kangaroo from the Oligocene-Miocene Etadunna Formation of Ngama Quarry, Lake Palankarinna, South Australia. *Australian Journal of Zoology,* 55:331-339.

Kear, B.P., Archer, M., and Flannery, T.F. 2001a. Postcranial morphology of *Ganguroo bilamina* Cooke, 1997 (Marsupialia: Macropodidae) from the middle Miocene of Riversleigh, northwestern Queensland. *Memoirs of the Association of Australasian Palaeontologists,* 25:123-138.

Kear, B.P., Archer, M., and Flannery, T.F. 2001b. Bulungamayine (Marsupialia: Macropodoidea) postcranial elements from the late Miocene of Riversleigh northwestern Queensland. *Memoirs of the Association of Australasian Palaeontologists*, 25:103-122.

Kear, B.P., Cooke, B.N., Archer, M., and Flannery, T.F. 2007. Implications of a new species of the Oligo-Miocene kangaroo (Marsupialia: Macropodoidea) *Nambaroo*, from the Riversleigh World Heritage Area, Queensland, Australia. *Journal of Paleontology,* 81:1147-1167.

Luckett, W.P. 1993. An ontogenetic assessment of dental homologies in therian mammals, p. 182-204. In Szalay, F.S., Novacek, M.J., and McKenna, M.C. (eds.), *Mammal Phylogeny: Mesozoic Differentiation, Multituberculates, Monotremes, Early Eutherians and Marsupials*. Springer-Verlag, New York.

Megirian, D., Prideaux, G.J., Murray, P.F., and Smit, N. 2010. An Australian land mammal age biochronological scheme. *Paleobiology*, 36:658-671.

Metzger, C.A. and Retallack, G.J. 2010. Middle Miocene climate change in the Australian outback. *Australian Journal of Earth Sciences*, 57:871-885.

Murray, P.F. 1989. The cranium of *Hadronomas puckridgi* Woodburne, 1967 (Macropodoidea: Macropodidae) a primitive macropodid kangaroo from the late Miocene Alcoota Fauna of the Northern Territory. *The Beagle,* 6:115-132.

Murray, P.F. 1991. The sthenurine affinity of the Late Miocene kangaroo, *Hadronomas puckridgi* Woodburne (Marsupialia, Macropodidae). *Alcheringa*, 15:255-283.

Prideaux, G.J. 2004. Systematics and evolution of the sthenurine kangaroos. *University of California Publications in Geological Sciences*, 146:i-xvii, 1-623.

Prideaux, G.J. and Warburton, N. M. 2010. An osteology-based appraisal of the phylogeny and evolution of kangaroos and wallabies (Macropodidae: Marsupialia). *Zoological Journal of the Linnean Society*, 159:954-987.

Simpson, G., Roe, A., and Lewontin, R. 1960. *Quantitative Zoology*. Harcourt Brace, New York.

Sorenson, M.D. and Franzosa, E.A. 2007. Treerot ver. 3.0. Department of Biology, Boston University, Boston, MA, 02215, USA.

Swofford, D.L. 2002. PAUP*. Phylogenetic Analysis Using Parsimony (*and Other Methods). Version 4 (updated to 10 beta). Sinauer Associates, Sunderland, Massachussets.

Szalay, F.S. 1969. Mixodectidae, Microsyopidae, and the Insectivore-Primate transition. *Bulletin of the American Museum of Natural History*, 140:193-330.

Tedford, R.H. and Woodburne, M.O. 1987. The Ilariidae, a new family of vombatiforme marsupials from Miocene strata of South Australia and an evolution of the homology of molar cusps in the Diprotodontia, p. 401-418. In Archer, M. (ed.), *Possums and Opossums: Studies in Evolution*. Surrey Beatty and Sons, Sydney.

Travouillon, K.J., Archer, M., Hand, S.J., and Godthelp, H. 2006. Multivariate analyses of Cenozoic mammalian faunas from Riversleigh, north-western Queensland. *Alcheringa*, Special Issue 1:323-349.

Travouillon, K.J., Legendre, S., Archer, M., and Hand, S.J. 2009. Palaeoecological analyses of Riversleigh's Oligo-Miocene Sites: Implications for Oligo-Miocene climate change in Australia. *Palaeogeography, Palaeoclimatology, Palaeoecology*, 276:24-37.

Travouillon, K.J., Escarguel, G., Legendre, S., Archer, M., and Hand, S.J. 2011. The use of MSR (Minimum Sample Richness) for sample assemblage comparisons. *Paleobiology*, 37:696-709.

Wible, J.R. 2003. On the cranial osteology of the short-tailed opposum *Monodelphis brevicaudata* (Didelphidae, Marsupialia). *Annals of Carnegie Museum*, 72:137-202.

Woodburne, M.O. 1984. *Wakiewakie lawsoni*, a new genus and species of Potoroinae (Marsupialia: Macropodidae) of medial Miocene age, South Australia. *Journal of Paleontology,* 58:1062-1073.

Worthy, T.H., Tennyson, A.J.D., Archer, M., Musser, A.M., and Hand, S.J. 2006. Miocene mammal reveals a Mesozoic ghost lineage on insular New Zealand, southwest Pacific. *Proceedings of the National Academy of Sciences of the United States of America*, 103:19419-19423.

APPENDIXES

For appendix material, see palaeo-electronica.org/content/2014/711-riversleigh-basal-macropodoids

APPENDIX 1. Measurements of the lower dentition of type and referred material of *Ganguroo bilamina* in mms. L – anteroposterior length, AW = anterior width, PW = posterior width, dp = deciduous premolar, p = premolar, m = molar.

APPPENDIX 2. Measurements of the upper dentition of type and referred material of *Ganguroo bilamina* in mms. L – anteroposterior length, AW = anterior width, PW = posterior width, dP = deciduous premolar, P = premolar, M = molar.

APPENDIX 3. Measurements of the lower dentition of type and referred material of *Ganguroo bites* in mms. L – anteroposterior length, AW = anterior width, PW = posterior width, dp = deciduous premolar, p = premolar, m = molar.

APPENDIX 4. Measurements of the lower dentition of type and referred material of *Bulungamaya delicata/'Nowidgee matrix'* in mms. L – anteroposterior length, AW = anterior width, PW = posterior width, dp = deciduous premolar, p = premolar, m = molar.

APPENDIX 5. Measurements of the upper dentition of type and referred material of *Bulungamaya delicata/'Nowidgee matrix'* in mms. L – anteroposterior length, AW = anterior width, PW = posterior width, dP = deciduous premolar, P = premolar, M = molar.

APPENDIX 6. Measurements of the lower dentition of additional specimens used in analyses, in mms. L – anteroposterior length, AW = anterior width, PW = posterior width, p = premolar, m = molar.

APPENDIX 7. Measurements of the uppers dentition of additional specimens used in analyses, in mms. L – anteroposterior length, AW = anterior width, PW = posterior width, P = premolar, M = molar.

APPENDIX 8. Univariate statistics of specimens of *Thylogale stigmatica*. N = number of specimen, Min = minimum measurement, Max = maximum measurement, L = anteroposterior length, AW = anterior width, PW = posterior width, p = lower premolar, P = upper premolar, m = lower molar, M = upper molar.

APPENDIX 9. Univariate statistics of specimens of *Thylogale thetis*. N = number of specimen, Min = minimum measurement, Max = maximum measurement, L = anteroposterior length, AW = anterior width, PW = posterior width, p = lower premolar, P = upper premolar, m = lower molar, M = upper molar.

APPENDIX 10. Univariate statistics of combined specimens of *Thylogale stigmatica and T. thetis*. N = number of specimen, Min = minimum measurement, Max = maximum measurement, L = anteroposterior length, AW = anterior width, PW = posterior width, p = lower premolar, P = upper premolar, m = lower molar, M = upper molar.

APPENDIX 11. Univariate statistics of type and referred material of *Ganguroo bilamina*. N = number of specimen, Min = minimum measurement, Max = maximum measurement, L = anteroposterior length, AW = anterior width, PW = posterior width, p = lower premolar, P = upper premolar, m = lower molar, M = upper molar.

APPENDIX 12. Univariate statistics of type and referred material of *Bulungamaya delicata/'Nowidgee matrix'*. N = number of specimen, Min = minimum measurement, Max = maximum measurement, L = anteroposterior length, AW = anterior width, PW = posterior width, p = lower premolar, P = upper premolar, m = lower molar, M = upper molar.

APPENDIX 13. Bivariate plots with convex hulls of lower dentition of *Thylogale stigmatica* and *T. thetis,* using anterior width. L – anteroposterior length, AW = anterior width, p = premolar, m = molar.

APPENDIX 14. Bivariate plots with convex hulls of lower dentition of *Thylogale stigmatica* and *T. thetis,* using posterior width. L – anteroposterior length, PW = posterior width, p = premolar, m = molar.

APPENDIX 15. Bivariate plots with convex hulls of upper dentition of *Thylogale stigmatica* and *T. thetis,* using anterior width. L – anteroposterior length, AW = anterior width, P = premolar, M = molar.

APPENDIX 16. Bivariate plots with convex hulls of upper dentition of *Thylogale stigmatica* and *T. thetis,* using posterior width. L – anteroposterior length, PW = posterior width, P = premolar, M = molar.

APPENDIX 17. Principle Component Analysis with convex hulls of upper (**1**) and lower (**2**) dentition of *Thylogale stigmatica* and *T. thetis.*

APPENDIX 18. Results of the Multivariate Analysis Of Variance (MANOVA) analysis showing the P-values for the mean comparison of upper (**1** and **3**) and lower (**2** and **4**) log transformed dental measurements of *Thylogale stigmatica* and *T. thetis,* with separation of sexes (**1** and **2**) and without separation (**3** and **4**)*.

APPENDIX 19. Canonical Variates Analysis with convex hulls of upper (**1** and **3**) and lower (**2** and **4**) log transformed dental measurements of *Thylogale stigmatica* and *T. thetis,* with separation of sexes (**1** and **2**) and without separation (**3** and **4**).

APPENDIX 20. Results of the Canonical Variates Analysis (CVA) reclassification using log transformed dental measurements of *Thylogale stigmatica* and *T. thetis,* with separation of sexes (**1**) and without separation (**2**).**1,** group 1 = *T. stigmatica* male; group 2 = *T. stigmatica* female; group 3 = *T. thetis* female; group 4 = *T. thetis* male; **2,** group 1 = *T. stigmatica*; group 2 = *T. thetis*. Incorrect reclassifications are highlighted in grey.

Results of the Canonical Variates Analysis (CVA) reclassification using log transformed dental measurements of *Thylogale stigmatica* and *T. thetis,* with separation of sexes (**1**) and without separation (**2**).**1,** group 1 = *T. stigmatica* male; group 2 = *T. stigmatica* female; group 3 = *T. thetis* female; group 4 = *T. thetis* male; **2,** group 1 = *T. stigmatica*; group 2 = *T. thetis*. Incorrect reclassifications are highlighted in grey.

APPENDIX 21. Nexus-formatted character matrix for the 29 taxa included in our phylogenetic analyses. Outgroup taxa was *Trichosurus vulpecula*. ? = missing data; - = inapplicable.